University of Alberta

Identification of a PITX2 interacting protein using a yeast two-hybrid screen of a human trabecular meshwork cDNA library

by

Michael Wilton Sharp 

A thesis submitted to the Faculty of Graduate Studies and Research in partial fulfillment of the requirements for the degree of *Master of Science*

in

Medical Sciences – Medical Genetics

Edmonton, Alberta

Fall 2004

Your file Votre référence
ISBN: 0-612-95852-3
Our file Notre référence
ISBN: 0-612-95852-3

Acknowledgements:

This thesis has by no means been a solo project. I would like to acknowledge my supervisory committee for their guidance and constructive criticism. In particular, I would like to thank Dr. Michael Walter who has been an excellent supervisor and remained patient, supportive and enthusiastic about my research. I would also like to thank our collaborator Dr. Jon R. Polansky for providing us with the human trabecular meshwork primary cell culture and RNA, and The Glerum Laboratory for technical assistance regarding yeast experiments.

Past and present members of the Ocular Genetics Laboratory have shaped my life in many positive ways. Thanks to: James for my training and teaching me that "every minute counts," Matt and Fred for 'Florida Rules', Ramsey for squash and sage advice, Tara for gum, Lijia for washing the velvets (and other help), Farideh and Sherry for keeping the lab running smoothly.

I'm also grateful to the Alberta Heritage Foundation for Medical Research for financial support through an appreciated graduate studentship.

Finally, I'd like to thank: my family for their unconditional love and support, Susie for stability and encouragement throughout the busy last leg of this degree, and, of course, God, from Whom all good things come.

Table of Contents:

List of Tables:

Chapter One: Introduction

Chapter Two: Materials and Methods

Chapter Three: Results

Chapter Four: Discussion

List of Figures:

Chapter One: Introduction

Chapter Two: Materials and Methods

Chapter Three: Results

Chapter Four: Discussion

Lists of Abbreviations:

3AT	3-amino-triazole
AA	amino acids
AD	activation domain
ARMD	age related macular degeneration
ARS	Axenfeld Rieger Syndrome
ASD	anterior segment dysgenesis
*att*B	bacterial attachment recombination site
*att*L	left attachment recombination site
*att*P	phage attachment recombination site
*att*R	right attachment recombination site
BLASTn	Basic Local Alignment Search Tool - nucleotide
BLASTp	Basic Local Alignment Search Tool - protein
BSA	bovine serum albumin
Ca++	calcium ion
cbEGF	calcium binding epidermal growth factor
CBP	CREB-binding protein
CLIM	cofactor of LIM
cDNA	complementary deoxyribonucleic acid
cfu	colony forming units
cM	centi-Morgans
Co-IP	co-immunoprecipitation
CYP1B1	cytochrome P450 1B1
DB	DNA binding domain
DMEM	Dulbecco's Modified Eagle's Medium
DNA	deoxyribonucleic acid
ECM	extracellular matrix
EFEMP1	EGF-containing fibulin-like extracellular matrix protein 1
EFEMP2	EGF-containing fibulin-like extracellular matrix protein 2
EGF	epidermal growth factor
FBLN	fibulin
FC	fibulin c-terminal domain
FISH	fluorescence *in situ* hybridization
5FOA	5-fluroorotic acid
FOXC1	forkhead box C1
G*α*M	goat-anti-mouse
GLC1	glaucoma 1 loci (open-angle glaucoma loci)
GLC3	glaucoma 3 loci (congenital glaucoma loci)
HA	haemagglutinin
HD	homeodomain
HDAC1	histone deactylase 1
HEPES	4-(2-hydroxyethyl)-1-piperazineethane sulfonic acid
HIS	histidine
HRP	horseradish peroxidase
HTM	human trabecular meshwork

HUGO	Human Genome Organization
IOP	intraocular pressure
IP	immunoprecipitation
kb	kilobasepairs
kDa	kiloDalton
LEU	leucine
M6PRBP	mannose 6 phosphate receptor binding protein
mg	milligram
MRCS	microcornea, rod cone dystrophy, cataract and posterior staphloma
mRNA	messenger ribonucleic acid
MYOC	myocilin
NNO1	nanophthalmos locus 1
OAR	orthopedia, aristaless, and rax
OMIM	online Mendellian inheritance in man
OPTN	optineurin
PACG	primary angle closure glaucoma
PAGE	poly-acrylamide gel electrophoresis
PBS	phosphate buffered saline
PCR	polymerase chain reaction
PIT-1	pituitary specific transcription factor 1
PITX2	pituitary homeobox transcription factor 2
PSORT	prediction of protein sorting signals and localization sites
RACE	rapid amplification of cDNA ends
RNA	ribonucleic acid
RT-PCR	reverse transcriptase polymerase chain reaction
SC	Schlemm's canal
SDS	sodium dodecyl sulfate
TBST	tris buffered saline with tween-20
TFs	transcription factors
Tip60	Tat interactive protein 60kDa
TM	Trabecular meshwork
TRP	tryptophan
UAS	upstream activating sequence
URA	uracil
URS	upstream repressor sequence
UTR	untranslated region
X-GAL	5-bromo-4-chloro-3-indolyl-beta-D-galactopyranoside
Xp	Xpress epitope
Y2H	yeast 2-hybrid

Chapter One: Introduction

Glaucoma

Glaucoma is a leading cause of blindness throughout the world (Quigley 1996; Quigley and Vitale 1997; Foster and Johnson 2001). It affects both sexes equally (Quigley 1996; Foster and Johnson 2001), but the age of onset and progression differs between races (Quigley 1996; Racette et al. 2003). Glaucoma therapy cost expenditures have been estimated at $1.56 billion per year (Tielsch 1993). Both the numbers of patients and health care costs in developed nations will increase with their aging populations. This makes glaucoma a devastating disease to both the patient and society.

Glaucoma is a disease of phenotypic and etiological variability. It is clinically described as the gradual loss of visual field starting from the periphery due to a characteristic damage of the optic nerve and retina causing an irreversible blindness. The vision loss related to glaucoma is caused by the death of retinal ganglion cells. Prognostic factors include age, race, and family (genetic) history and an increased intra ocular pressure (IOP). An increase in IOP can lead to the cupping of the optic nerve head associated with glaucoma. Elevated IOP is a common risk factor of glaucoma.

In a normal eye, the aqueous humour is created by the ciliary body to clear debris from the lens and provide the lens with nutrients. The aqueous humour flows from the ciliary body and into the anterior chamber through the pupil (figure 1-1). The aqueous humour is then drained through the trabecular meshwork (TM) located at the vertex of the irideocorneal angle (figure 1-2a). The balance between creation and drainage of aqueous humour is integral in maintaining a certain intraocular pressure. If the aqueous humour cannot drain properly, the pressure can be inflated.

The Trabecular Meshwork

Playing a prominent role in the IOP homeostasis is the TM. The TM is the primary drainage route of the aqueous humour. The aqueous humour flows through the TM into the Schlemm's canal (SC) to leave the eye (figure 1-2a). The uveal face

of the TM appears porous with TM cells forming trabecular beams called trabeculae (figure 1-2b). The areas between the cells get progressively smaller towards the SC.

There are no cures for glaucoma, as the visual field loss is irreversible, but there are treatments that slow the vision loss and save remaining vision by alleviating IOP. Surgeries for prevention of further glaucotomous vision loss involve creating artificial aqueous humour drainage pathways to relieve IOP when the angle is blocked (figure 1-1b). These surgeries, called trabeculoplasty and trabeculectomy, demonstrate the crucial role of the TM in IOP maintenance and glaucoma pathogenesis. Medications used to treat glaucoma decrease IOP by opening the HTM, increasing aqueous outflow through secondary drainage routes or decreasing aqueous humour production from the ciliary body. Again, the function of the TM is to regulate aqueous humour outflow and decreased aqueous humour outflow can lead to elevated IOP and glaucoma.

HTM gene expression

Aqueous humour drainage is an active process that requires secretory, phagocytic, contractility and stress responsive properties of trabecular meshwork cells. A regulation of gene expression is required to govern these properties (Borras 2003). Gene expression in the human trabecular meshwork (HTM) is extremely diverse. Extensive genetic profiling of TM cDNA libraries has revealed a varied expression profile with low levels of gene redundancy (Gonzalez et al. 2000; Wirtz et al. 2002; Tomarev et al. 2003). Approximately 90% of transcripts are present at 0.1% with no transcripts expressed at greater than 2% of the transcriptome (Borras 2003). This diversity is representative of the multiple mechanisms the TM uses to regulate aqueous humour outflow.

One of these outflow mechanisms places the extracellular matrix (ECM) of the TM in an important role for regulating aqueous humour drainage. The size of the gaps visible between the trabeculae of the TM (figure 1-1b) does not correspond to the aqueous humour drainage rate calculations. Actual outflow is two orders of magnitude lower than expected (Ethier et al. 1986). In fact, most of these holes are filled with an extracellular matrix containing secreted proteins encoded and highly

expressed by trabecular meshwork cells (Acott et al. 1985; Gonzalez et al. 2000; Gong et al. 2002; Wirtz et al. 2002; Tomarev et al. 2003). Changes in the ECM distribution and contents is thought to affect and regulate aqueous humour outflow rates (Alexander et al. 1991). Abnormal turnover or accumulation of ECM proteins is related to outflow resistance and glaucoma (Borras 2003).

The TM therefore performs the important function of IOP maintenance via different mechanisms. The diverse genes expressed in the TM are important for its function. The HTM gene expression can be transcriptionally regulated by transcription factors expressed in the HTM. Alterations in gene expression can lead to decreased aqueous humour outflow, increased IOP, and glaucoma.

HTM cell culture

There are inherent difficulties in studying the HTM. The tissue is only millimeters wide and is difficult to remove or isolate quickly (figure 1-1b). Molecular biology studies are especially problematic due to the difficulty in obtaining fresh human ocular tissue for RNA or protein experiments before molecular degradation occurs.

TM studies have been accomplished by taking the small amount of HTM tissue available and creating primary cell cultures or immortalized cell lines to be used for further studies (Polansky et al. 1979). Morphological and growth characteristics of HTM cells in culture make them distinguishable from cells of neighboring, possibly contaminating, tissues. Performed properly, HTM cell culture acts as a good model for studying normal and glaucomatous tissue in reproducible experimental conditions (Polansky et al. 1984). HTM cell culture, therefore, can be an appropriate and valuable tool for studying the HTM, aqueous humour outflow and glaucoma pathogenesis.

Glaucoma Genetics

By identifying glaucoma early, vision loss can often be prevented. Because of the genetic aspect of glaucoma, research in this field can help lead to early disease detection through genetic testing and pre-symptomatic screening methods. When

glaucoma loci and genes are identified, more in-depth research into the understanding of molecular mechanisms and pathogenesis can lead to better glaucoma treatments and possibly cures. The genetics and molecular biology of glaucoma are complex, not well understood, and are open for further discovery (Friedman and Walter 1999).

To date, there have been seven genetic loci identified for open angle glaucoma (GLC1A-G) and three loci for congenital glaucoma (GLC3A-C) (table 1-1). Of these loci, corresponding disease genes have been identified for three. Mutations in *MYOC* at GLC1A, *OPTN* at GLC1E, *CYP1B1* at GLC3A have been found (Stoilov et al. 1997; Stone et al. 1997; Rezaie et al. 2002). Summaries of candidate genes for the other glaucoma loci are available (Gonzalez et al. 2000; Wentz-Hunter et al. 2002; Borras 2003; Tomarev et al. 2003) Most glaucoma genes remain to be identified.

All of the known glaucoma genes (*MYOC*, *OPTN*, *CYP1B1*) are expressed in the human trabecular meshwork (Tomarev et al. 2003). Mutations in these genes could cause altered HTM function, leading to an increased IOP and glaucoma.

The knowledge base of glaucoma genetics is limited. The genetic variability of glaucoma suggests the existence of multiple disease mechanisms, none of which are currently well understood.

Axenfeld-Rieger Syndrome

Axenfeld-Rieger Syndrome (ARS) describes several overlapping glaucoma-related phenotypes caused by multiple genetic loci (Alward 2000). ARS encompasses the previously separate, but genotypically and phenotypically related Axenfeld anomaly, Rieger anomaly, iridogoniodysgenesis anomaly, Axenfeld syndrome, Rieger syndrome, iridogoniodysgenesis syndrome.

ARS is a rare congenital phenotype inherited in an autosomal dominant fashion with high penetrance. ARS includes several ocular abnormalities that are sometimes associated with dental and umbilical anomalies (figure 1-3) (Semina et al. 1996). ARS ocular abnormalities are anterior chamber defects that can include a displaced Schwalbe's line, corectopia, iris hypoplasia, and iris coloboma. The cellular lineages of affected tissues in ARS are of a common neural crest origin that includes the trabecular meshwork (Lines et al. 2002). The anterior angle dysgenesis

can lead to an increased IOP and subsequently, glaucoma. Over half of ARS patients will suffer from an early onset secondary glaucoma (Shields et al. 1985).

PITX2

Mutations in PITX2 cause ARS

ARS can be caused by mutations in the pituitary homeobox transcription factor 2 (PITX2) gene at 4q25-26. A wide range of different PITX2 mutations are associated with ARS. These mutations vary from insertions, frameshift mutations, missense mutations and nonsense mutations, as well as whole gene deletions (figure 1-4) (Lines et al. 2004). These mutations model haploinsufficiency, over-expression and dominant negative mutation mechanisms and there is also range of ocular phenotype severity. A putative genotype to phenotype correlation exists in which lower wildtype PITX2 function results in more severe ocular phenotypes (Kozlowski and Walter 2000). These mutations suggest multiple mechanisms of ARS pathogenesis through PITX2 mutations.

Pitx2 expression in the eye is shown in ARS affected precursor tissues at day E11.5 in mouse (Hjalt et al. 2000). Mice homozygous for Pitx2 mutations die at day 10 with severe cardiovascular malformations (Gage et al. 1999; Lin et al. 1999; Lu et al. 1999). A small subset (10%) of heterozygous mice have iris malformation phenotypes (Gage et al. 1999). The findings that mutations in human and mouse PITX2 cause ocular defects demonstrate the importance of PITX2 in the developing and adult eye.

PITX2 is a transcription factor

PITX2 is a bicoid-like, paired class, homeobox transcription factor (Semina et al. 1996). PITX2 contains two known protein domains (figure 1-4). A homeodomain exists near the N-terminal end and an OAR domain is located near the C-terminus. The homeodomain is a structured, 60 amino acid, DNA binding domain. A lysine residue at position 50 in the homeodomain specifies PITX2's DNA binding site and classifies PITX2 as a bicoid-like transcription factor (Hanes and Brent 1989). The PITX2 homeodomain recognizes and binds the 5'-TAATCC-3' sequence in DNA

(Amendt et al. 1998). The OAR domain is a 15-20 AA region conserved in certain transcription factors and is named for the initials of orthopedia, aristaless, and rax (retina and anterior neural fold) transcription factors in which this domain was first identified (Furukawa et al. 1997).

PITX2 can regulate gene expression in the TM

As a transcription factor, PITX2 is able to regulate the gene expression of tissues in which PITX2 is expressed. Among other tissues, PITX2 is expressed in the human fetal eye, (EST data, UniGene), the infant HTM (Wirtz et al. 2002) and the adult HTM (Tomarev et al. 2003). PITX2 is highly expressed in the adult HTM (Tomarev et al. 2003) suggesting PITX2 could have a role in maintenance of the TM and drainage pathway in glaucoma pathogenesis. Expression of PITX2 in fetal, infant and adult ocular tissues suggests both developmental and adult roles for PITX2. As a transcription factor in the trabecular meshwork, PITX2 can help regulate gene expression necessary for TM function and therefore maintain IOP.

One way that PITX2 can affect TM function by gene regulation is through cellular proliferation. Pitx2 is a component of the Wnt/Dvl/β-catenin pathway and has a role in cellular proliferation (Kioussi et al. 2002). Pitx2 serves as a transcriptional regulator in the G1 phase of the cell cycle. The DNA binding ability of Pitx2 and the N-terminal domain of the Pitx2 protein are required for this cell cycle effect. The authors propose that Pitx2 acts as a tissue-specific transcription factor in the common Wnt/Dvl/β-catenin pathway to regulate the cell cycle.

Cellular proliferation is an important mechanism in the function of the TM. A loss of trabecular beams due to depletion of TM cells has been associated with glaucoma and it is postulated that this cellularity in the TM is important for proper outflow maintenance (Alvarado et al. 1984; Polansky et al. 1984). Regulating cellular proliferation through gene expression is one way PITX2 could affect TM function and IOP management.

PITX2 interacts with other proteins to regulate transcription

There is an important role for protein-protein interactions in homeodomain protein activity. Interactions can allow the stimulation (Bach et al. 1997; Bradford et al. 1997; Durocher et al. 1997; Tremblay et al. 1998) or inhibition (Stark and Johnson 1994; Hassan et al. 1997; Zhang et al. 1997; Tolkunova et al. 1998) of transcriptional activity (figure 1-5). Interactions can also allow transcription factors to have alternate functions as transcriptional activators or repressors dependent upon promoter context and cellular conditions (Pinsonneault et al. 1997; Xu et al. 1998; Scully et al. 2000).

The homeodomain of PITX2 can bind DNA alone, but it does not have a transactivation function (Amendt et al. 1999). This demonstrates that PITX2 transcriptional activation domains outside of the homeodomain. It is probable that the transcriptional activation domains act through protein-protein interactions to regulate transcription.

PITX2 can interact with other proteins and with itself (Amendt et al. 1999; Saadi et al. 2003). PITX2-PITX2 homodimerization was originally thought to occur through the homeodomain (Amendt et al. 1999), but a yeast two-hybrid study demonstrated that PITX2 dimerization requires both the homeodomain and C-terminal tail (Saadi et al. 2003). While PITX2 dimerization is DNA independent *in vitro*, the PITX2 dimer is able to bind DNA and is more stable than the monomer on DNA (Saadi et al. 2003). The exact dimerization model remains controversial (Matthew Lines personal communication).

PITX2 also interacts with the pituitary specific transcription factor PIT-1 independent of DNA (Amendt et al. 1998). The interaction occurs through the C-terminal region of PITX2 that includes the PITX2 OAR domain. The PITX2/PIT-1 interaction also affects the transactivational function of PITX2 by alleviating a PITX2 intramolecular auto-inhibititory interaction (Amendt et al. 1999). The PITX2/PIT-1 interaction is negated by some of the PITX2 ARS mutations (Saadi et al. 2003). PIT-1 is only expressed in the pituitary gland, therefore, this specific interaction would only occur in the pituitary. However, the PITX2/PIT-1interaction has been postulated to be prototypic of transcriptional regulatory interactions that occur in other tissues like the trabecular meshwork (Amendt et al. 1998).

PITX2 interacts with HDAC1, TIP60, CBP/p300, CLIM, and β-Catenin in a temporally specific manner (Kioussi et al. 2002). These coactivators are recruited by PITX2 to a promoter for transcriptional activation. Recently, PITX2 has also been shown to interact with FOXC1 (Matthew lines personal communication). *FOXC1* is another ARS related gene that maps to 6p25 (Larsson et al. 1995; Mears et al. 1996; Mears et al. 1998). It is a winged-forkhead transcription factor that has transcriptional activation domains at both termini and an internal inhibitory domain (Berry et al. 2002). Like PITX2, FOXC1 is expressed in the developing eye and adult trabecular meshwork (Mears et al. 1998; Kidson et al. 1999). The PITX2/FOXC1 interaction demonstrates that ARS related proteins physically interact with each other. This interaction can have important affects on gene regulation in the trabecular meshwork and aqueous humour outflow.

PITX2 is involved in several protein-protein interactions that can affect its function. These interactions can help regulate important gene expression in the TM and have a role in aqueous humour outflow and glaucoma pathogenesis. Further identification of PITX2 interacting partners will continue to define PITX2's biological role and involvement in ARS.

Unidentified ARS genes

ARS is genetically heterogeneous (figure 1-6). It has been estimated that 60% of ARS patients do not have PITX2 or FOXC1 mutations (Matthew Lines and Michael Walter, personal communication). Therefore, other ARS related genes exist. Aside from PITX2 and FOXC1, three other ARS loci have been identified. A locus at 13q14 (OMIM *601499) has been identified and named RIEG2 (Phillips et al. 1996). Other ARS loci exist on chromosome 16 (Werner et al. 1997) and the X chromosome (OMIM: 308500). Genes for these three loci have not been cloned. Because ARS related proteins have been shown to interact with each other (Lines and Walter, unpublished data), it is possible that ARS genes at these loci can be identified by discovering protein interacting partners of PITX2 and FOXC1.

Protein-Protein interactions

Many proteins in the cell interact with other proteins to function. Protein-protein interactions are involved in cell structure, DNA replication, transcription initiation, and many other processes. Specific protein-protein interactions can affect protein stability, localization and function. Post-translational modifications of proteins involve transient protein-protein interactions. As an example, protein kinases and protein phosphatases interact with their substrate proteins to determine their phosphorylation state and regulate their function. Protein-protein interactions are also involved in recruiting and assembling transcription complexes to regulate gene expression. By identifying a protein's interacting partners, clues to that proteins role in the cell can be uncovered. Identification of protein-protein interactions involving glaucoma and ARS genes will allow further understanding of the cellular roles of their encoded proteins. Identification of PITX2-protein interactions can aid in understanding the role of PITX2 in the cell.

PITX2 interacting proteins can be identified with a two-hybrid method

Several different experimental methods are available to identify or confirm PITX2 protein-protein interactions. These methods include co-immunoprecipitation, protein affinity chromatography, and affinity blotting (Phizicky and Fields 1995). One way to identify novel PITX2 interacting proteins is by screening a library using a two-hybrid system (Fields and Song 1989; Chevray and Nathans 1992) . The yeast two-hybrid (Y2H) system is an *in vivo* genetic system that detects protein-protein interactions occurring within a living cell. Since the advent of the yeast two-hybrid system, commercial versions have become available and thousands of protein-protein interaction studies have used this method. More specifically, protein-protein interactions relevant to ocular diseases have been identified using the yeast two hybrid screens (Wentz-Hunter et al. 2002; Klenotic et al. 2004). The yeast two-hybrid system has become an established method that can be used to test, identify, and characterize protein-protein interactions.

The Y2H system takes advantage of the *Saccharomyces cerevisiae* transcription factor, GAL4. GAL4 has modular DNA binding (DB) and

transcriptional activation domains (AD) that can be physically separated. The coding sequence of a protein of interest is fused in frame with the GAL4 –DB coding sequence to create a fusion protein (figure 1-7). This fusion protein will bind the GAL4 DNA target sequence upstream of a reporter gene and act as *bait* to trap interacting proteins. The *prey* proteins to be trapped are encoded by the GAL4-AD sequence fused in frame with a cDNA library. GAL4 function is reconstituted when the DB and AD are brought together in close proximity by a bait/prey interaction and the reporter gene is activated. Activation of the reporter gene allows the identification of clones encoding interacting proteins.

There are certain considerations to be taken into account when designing a two-hybrid screen. In order to increase the chances of identifying a biologically relevant interaction, the bait protein should be tested against prey proteins that are expressed in a common tissue. Because PITX2 is highly expressed in HTM cells, and HTM gene expression is important in IOP regulation and glaucoma pathogenesis, trabecular meshwork cells are an ideal starting material for a yeast two-hybrid library.

Bait proteins can also mimic an interaction phenotype if the bait has its own transcriptional activation domain. In this case, the bait protein will activate reporter gene expression in the absence of an interacting prey protein and produce false positives. Because PITX2 is a transcription factor, a PITX2-DB bait protein may self-activate. This problem can be addressed by assaying PITX2-DB transcriptional self-activation and designing deletion constructs to remove PITX2 transcriptional activation domains if necessary.

The cellular environment in yeast differs from that of an HTM cell. For example, PITX2-DB and the prey proteins could be post-translationally modified differently than in a human cell. Because the two-hybrid PITX2/prey interactions are occurring within yeast, an identified interaction may not reflect an endogenous mammalian situation. To address this problem, interactions identified by the yeast two-hybrid system need to be re-assessed and verified within a mammalian system. If the proper considerations are taken into account, a yeast two-hybrid cDNA library screen is an established, reliable system that can be used for identification of PITX2 protein-protein interactions.

Research project description

I hypothesize that PITX2 interacts with other proteins to function. I further hypothesize that by identifying PITX2 protein-protein interactions I can identify ARS and glaucoma related candidate genes. These protein-protein interactions will be identified through a yeast two-hybrid screen of an HTM cDNA library. Putative protein-protein interactions will be confirmed in a mammalian system to model biological protein folding and post-translational modifications. Validated PITX2 interacting partners will serve as candidate genes for glaucoma and developmental ocular disorders like ARS.

A)

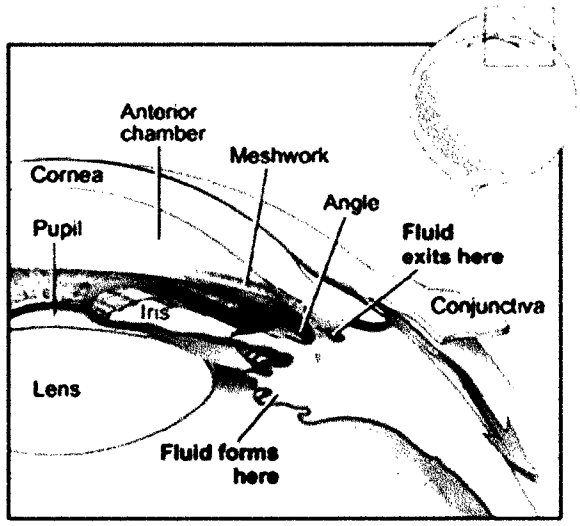

B)

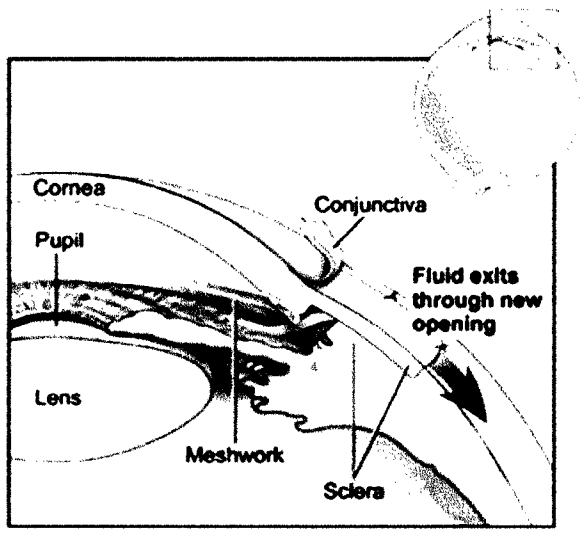

A)

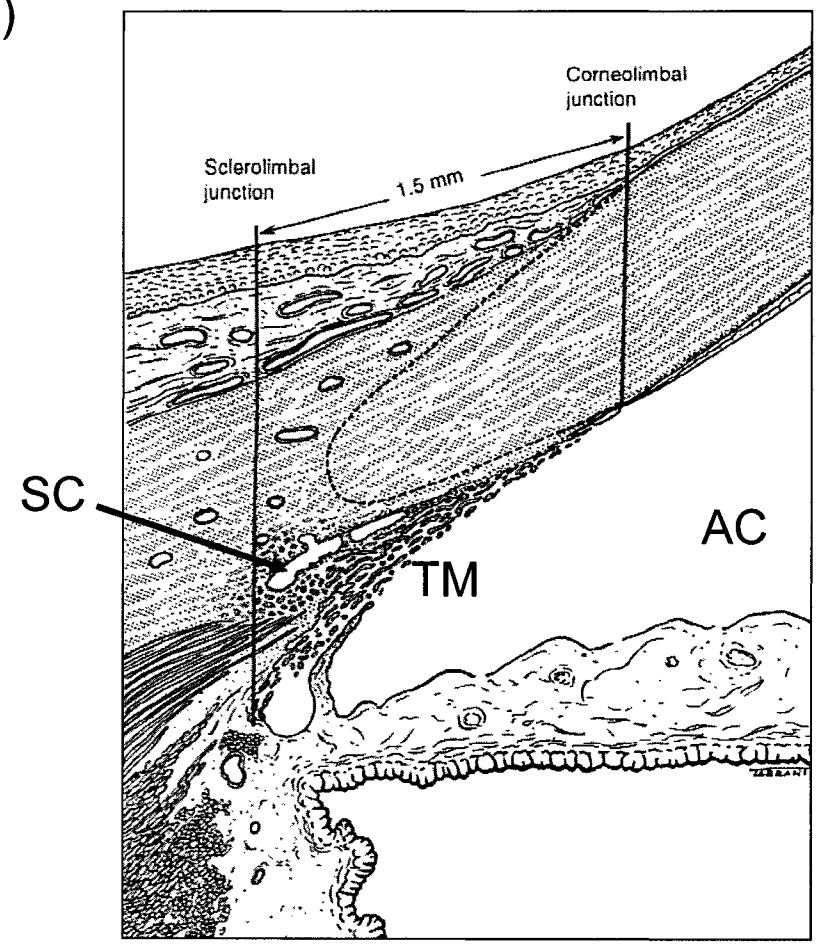

B)

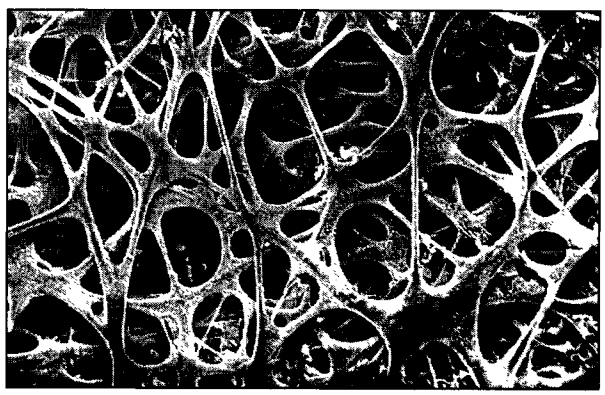

Table 1-1: Glaucoma loci and genes

Locus	Location	Gene	References
GLC1A	1q21-1q23	*MYOC*	(Sheffield et al. 1993) (Stone et al. 1997)
GLC1B	2cen-q13		(Stoilova et al. 1996)
GLC1C	3q21-q24		(Wirtz et al. 1997)
GLC1D	8q23		(Trifan et al. 1998)
GLC1E	10p15-14	*OPTN*	(Sarfarazi et al. 1998) (Rezaie et al. 2002)
GLC1F	7q35-q36		(Wirtz et al. 1999)
GLC1G	5q15-5q22		(Samples et al. *IOVS* 2004; ARVO E-Abstract 4622)
GLC3A	2p21	*CYP1B1*	(Sarfarazi et al. 1995) (Stoilov et al. 1997)
GLC3B	1p36.2-p36.1		(Akarsu et al. 1996)
GLC3C	14q24.3		(Stoilov et al. *IOVS* 2002;43: ARVO E-Abstract 3015)

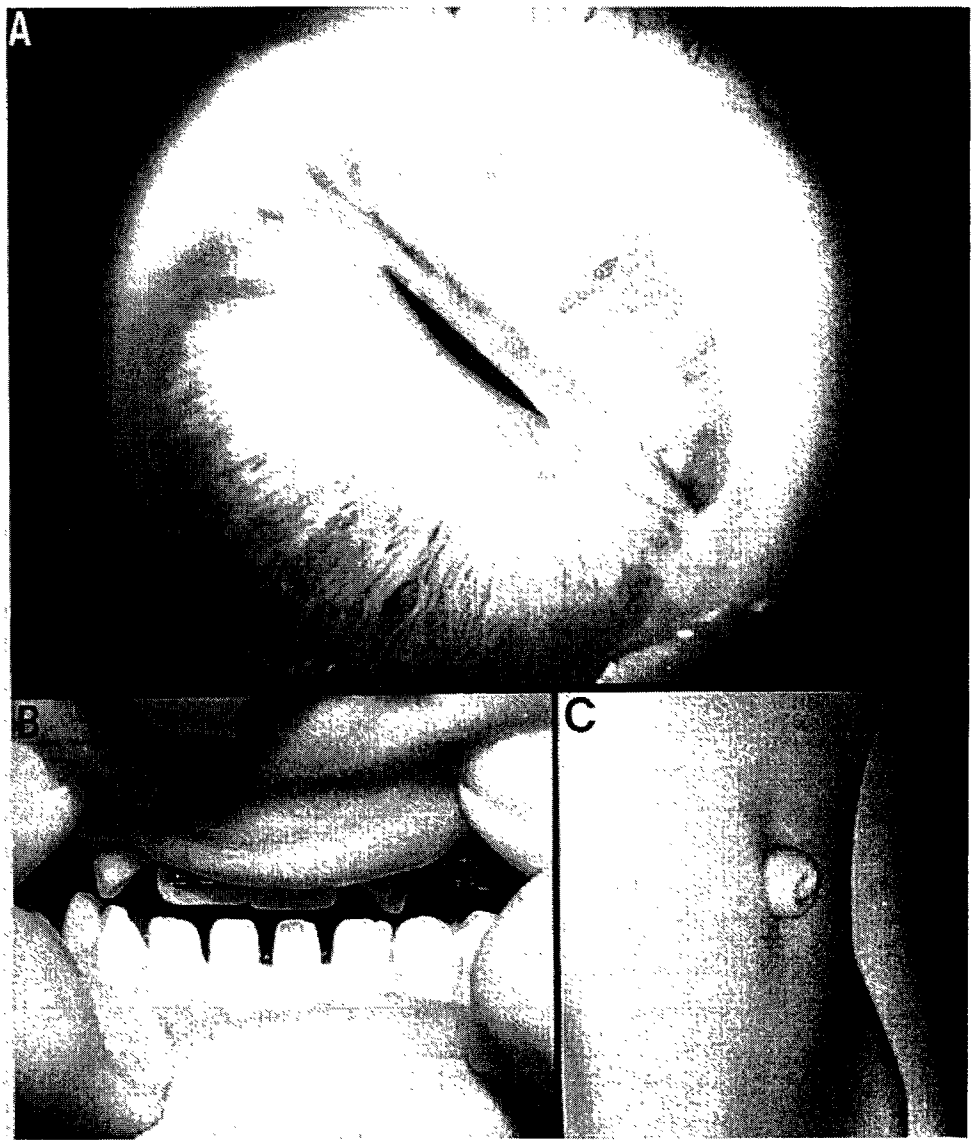

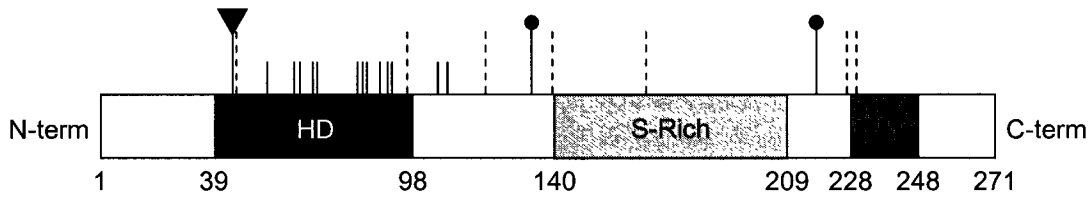

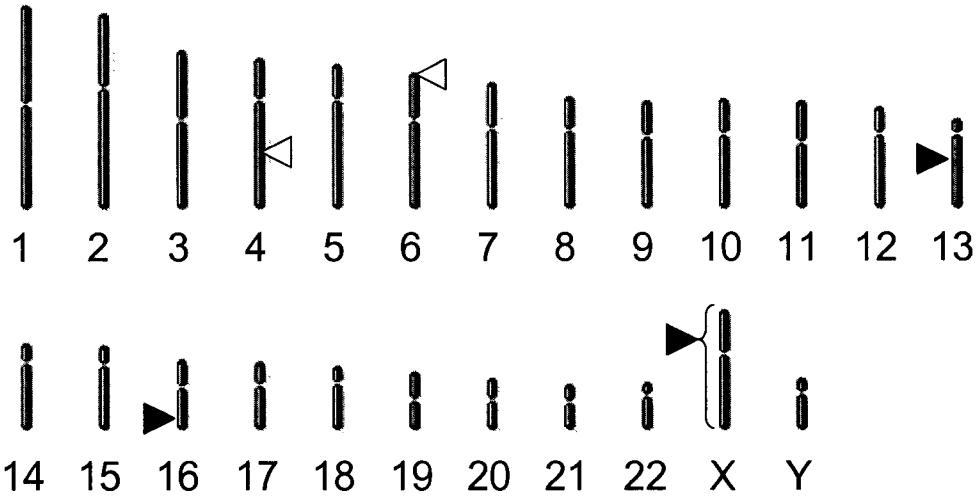

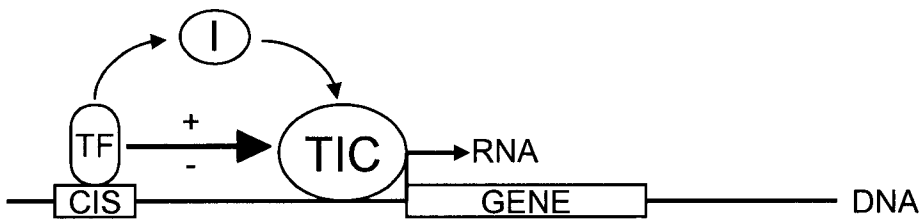

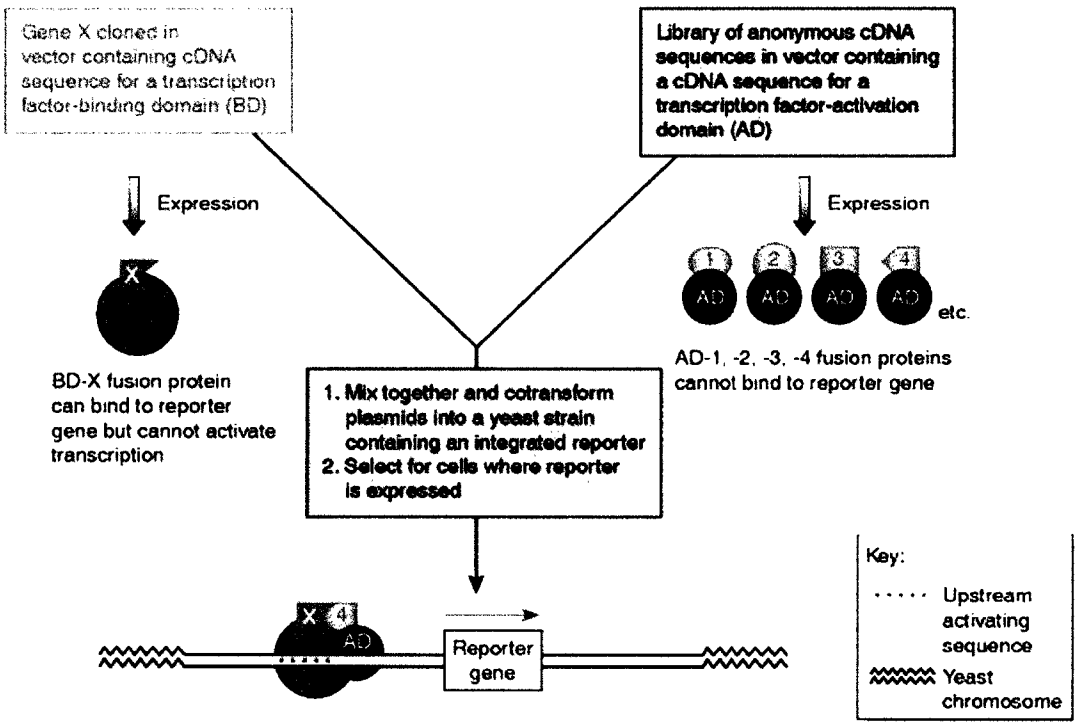

Chapter Two: Materials and Methods

1) Creation of a CytoTrap Y2H porcine cDNA library

Porcine tissue dissection and RNA isolation

Six pig eyes were collected from Olymel Pork Slaughterhouse and Cutting Plant, Red Deer, less than one hour post mortem. The peri-ocular muscles were removed and the anterior chamber was separated from the rest of the eye. The anterior chamber tissues were placed in RNA*later* Tissue Collection: RNA Stabilization Solution (Ambion, Inc.) and placed on ice until more fine-scale dissection could be done. The anterior angle (including trabecular meshwork, Schlemm's canel and the ciliary body) was separated from the cornea and iris using a dissection microscope. Five hundred milligrams of angle tissue were homogenized in 10 mL of TRIzol reagent (Invitrogen) and total RNA was extracted following the manufacturer's recommendations. The total RNA was subsequently enriched for poly-A RNA using the Oilgotex mRNA purification system (QIAGEN).

Modified cDNA synthesis protocol

Five micrograms of poly-A enriched RNA was used for radiolabeled first and second strand synthesis in the CytoTrap XR Library Construction kit (Stratagene). The cDNA termini were blunted and ligated with a modified *Eco*RI adapter (figure 2-1). The *Eco*RI adapter was modified to include the sequence of a Gateway-compatible *att*B1 site (Invitrogen). To create the adapter, the forward and reverse oligomers were mixed at a 1:1 molar ratio in water, heated to 95°C for one minute and allowed to anneal slowly at room temperature overnight. Following the cDNA/adapter ligation, the *Eco*RI ends where phosphorylated and the 3' *Eco*RI end was removed by *Xho*I digestion.

Modification of CytoTrap prey vector

Mutagenesis (QuikChange Site-Directed Mutagenesis Kit Stratagene) was used to incorporate an *att*B2 site into the pMyr prey vector (Stratagene) as per the manufacturer's recommendations. See figure 2-1 for mutagenic primer sequences. Clone DNA was manually sequenced with the 5' Myr primer and using the ^{33}P-

radiolabeled terminator ThermoSequenase Cycle Sequencing Kit (Amersham Biosciences) to confirm the mutation. See table 2-1 for sequencing primer sequence. The modified and sequenced region was sub-cloned back into a wild type vector backbone to eliminate the possibility of secondary mutations.

Ligations and Transformations

Size fractionated cDNA samples were quantified on ethidium bromide plates, and the cDNA was ligated into the modified pMyr vector as per CytoTrap manual. Bacterial transformations were done using XL10-Gold Kan Ultracompetent cells (Stratagene) with the recommended protocol and then plated appropriately.

Gateway-compatible site confirmation

Small scale plasmid DNA preparations (QIAGEN) were made from ten randomly picked colonies and analyzed by restriction digests to confirm presence of cDNA inserts. Three clones were sequenced with an automated LI-COR DNA sequencer. See table 2-1 for primer sequence. To test the function of the *att*B sites, a Gateway BP recombination reaction (Invitrogen) was performed on a select clone and a pDONR 201 vector (Invitrogen) (gift from Glerum lab). A BP reaction mediates recombination though an *att*B (bacterial attachment) and an *att*P (phage attachment) λ phage recombination sites in the vectors that flank the DNA sequence to be exchanged. The BP reactions were transformed into bacteria and plated. Restriction analysis was used to confirm insert shuttling.

2) Custom built HTM ProQuest cDNA library

Our collaborator, Dr. Jon R. Polansky, provided us with total RNA isolated from a human trabecular meshwork (HTM) primary cell culture created from a 30yr old non-glaucomatous donor. The culturing method is as described (Polansky et al. 1979; Polansky et al. 1984). The RNA extraction was performed by standard methods. Poly-A enriched RNA was isolated from 100 μg of total RNA using QIAGEN Oligotex as above.

Library Characteristics

The HTM yeast two-hybrid cDNA library was created by Invitrogen and contained $2.1x10^6$ primary colony forming units before semi-solid amplification and $7.8x10^9$ cfu in the amplified library. Twenty-four independent primary clones were analyzed. Of these, 23 contained cDNA inserts (96% of total) with an average insert size of 1.9kb. The library was directionally cloned into the pEXP-AD502 ProQuest yeast two-hybrid prey vector (Invitrogen) using a *Not*I adapter on the oligo-dT primer and 5' blunt end ligation into the vector's *Eco*RV site. The *Eco*RV site was destroyed in the library plasmid DNA because the cDNA inserts do not contain the complementary *Eco*RV recognition sequence.

Plasmid isolation

I inoculated 250mL of LB media with $2.5x10^9$ cfu of the HTM library and grew the culture overnight at 30°C. Plasmid DNA was isolated as in ProQuest pre-made cDNA library manual (Invitrogen). Three micrograms of the plasmid DNA was digested with *Bsr*GI (New England Biolabs) to confirm insert average size and size range. Standard PCR was performed on 50 ng of the library plasmid DNA with the full length PITX2 *att*B primer set (table 2-1).

3) HTM Y2H library screen using PITX2 as bait

PITX2 bait construct creation and self-activation titration

A full length PITX2 bait construct was created to include the full 271 amino acid PITX2 open reading frame. The PITX2 homeodomain (HD) construct encodes the entire homeodomain and six more amino acids on either end (amino acids 33-104, inclusive). Both constructs were designed without stop codons in anticipation of using Gateway shuttling to create C-terminal fusion proteins for downstream applications. There are stop codons in all three frames immediately following the *att*B2 site in the pDEST-32 vector that terminate bait fusion proteins. FailSafe PCR (EPICENTRE) was used to amplify full length PITX2 and the PITX2 homeodomain

from a pcDNA-PITX2 construct (provided by Tim Footz). See table 2-1 for primer sequences. The PCR amplicons were gel extracted (QIAGEN) and Gateway shuttled through a BP reaction with pDONR 221 (Invitrogen) to create an entry clone (figure 2-2). Entry clone plasmid DNA was isolated by a small scale DNA preparation (QIAGEN) and recombined with pDEST-32 in an LR Gateway recombination reaction (Invitrogen). An LR reaction mediates recombination though the *att*L (left attachment) and *att*R (right attachment) phage based recombination sites flanking the DNA sequence to be exchanged. The LR reaction created the expression clones. The expression clone inserts were sequenced with Applied Biosystems (ABI) automated DNA sequencers and the junctions were sequenced manually as described above. Large-scale DNA preparations (QIAGEN) of both constructs were carried out. Bait protein self activation was tested as in the manufacturer's ProQuest protocol (Invitrogen).

Co-Transformation of PITX2 and cDNA library

Ten micrograms of the full length PITX2 bait construct was co-transformed with 10μg of isolated library DNA into the MaV203 (*MAT*α) yeast strain. Yeast co-transformations and plating were performed as recommended (ProQuest, Invitrogen). Selection plates were incubated at 30°C and monitored daily for seven days.

Assessment of interactions within Y2H system

Co-transformed colonies growing on media lacking leucine (LEU), tryptophan (TRP), and histidine (HIS) were picked and streaked onto plates lacking LEU and TRP to isolate single purified colonies from the original. Four colony isolates per original colony were streaked onto master plates (-LEU-TRP) along with the yeast control strains in the pattern suggested in the Proquest manual. Replica plating and replica cleaning onto the four assay media were done as suggested. Following the appropriate incubation and the X-gal assay, colonies presenting a putative interaction phenotype were selected for further analysis.

Interacting prey sequence identity determination

Bait and prey plasmid DNA were recovered from yeast and transformed into bacteria using electroporation of ElectroMAX DH10B cells (Invitrogen) or XL10-Gold Kan Ultracompetent cells (Stratagene) with recommended protocols. The transformations were plated on media containing gentamicin to recover the bait plasmid or ampicilin to isolate the prey plasmid. Small-scale DNA preparations (QIAGEN) were performed on multiple bacterial clones for each yeast clone. *Bam*HI digests were used to compare the original and recovered bait constructs. A *Bsr*GI digest of the recovered prey construct identifies cDNA insert presence and size. Prey bacterial DNA preps with cDNA inserts were sequenced with ABI automated DNA sequencers, using pEXP-AD502 forward and reverse primers (table 2-1). Prey cDNA insert sequences were submitted to the BLASTn program at NCBI (http://www.ncbi.nlm.nih.gov/BLAST/) to reveal identity.

Confirmation of interaction within Y2H system

The re-transformation assay described in the ProQuest manual was performed for the 2P152 and 2P141 prey constructs. These prey constructs were also co-transformed with the PITX2 homeodomain bait construct and a full length FOXC1 bait construct provided by Lijia Huang.

4) EFEMP2 in silico normal tissue expression profile

EFEMP2 tissue expression profile was determined by the SOURCE program at http://source.stanford.edu.

5) PITX2 dimerization interaction in the Y2H system

A LR Gateway recombination reaction was used to move the full length PITX2 entry clone insert into the prey vector pDEST-22. The reading frame of the insert was confirmed by ABI sequencing with vector primers (table 2-1). The self-activation of this construct was titrated as recommended. The PITX2 bait and PITX2 prey constructs were co-transformed into yeast and four independent, isolated, co-

transformant colonies were picked and their reporter phenotypes were assayed as above.

6) PITX2-EFEMP2 interaction in mammalian system

Creation of an EFEMP2 mammalian expression construct

A BP Gateway reaction of the 2P152 prey plasmid DNA and pDONR 221 created an EFEMP2 entry clone. This EFEMP2 clone is deleted for the 36 N-terminal amino acids of EFEMP2 and will be referred to as $EFEMP2_{\Delta N36}$. The $EFEMP2_{\Delta N36}$ mammalian expression clone was constructed using an LR reaction of the 2P152 Entry Clone with the pcDNA3.1/nV5-DEST vector (Invitrogen). The expression clone contains an N-terminal V5 epitope tag. Correct transfer of the open reading frame was confirmed with ABI sequencing.

Preparation of whole cell lysates

COS-7 (adult male African green monkey kidney derived cell line) cells were maintained in Dulbecco's Modified Eagle's Medium (DMEM) with 10% fetal bovine serum (FBS) in 5% CO_2 at 37°C by May Yu. Ten centimeter plates were seeded with 10^6 cells 24 hours prior to transfection.

The V5-$EFEMP2_{\Delta N36}$ construct was co-transfected with an Xpress-PITX2 encoding construct in pcDNA HIS-MAX (created by Tim Footz) using 5 μg of DNA (2.5 μg per construct) in 24ul of Fugene 6 (Roche) and 776 ul of DMEM per 10cm plate. The cells were harvested three days subsequent to transfection. All reagents and tubes were kept on ice. The culture media was removed and the cells were rinsed in phosphate buffered saline (PBS) pH 7.2 (137 mM NaCl, 2.7 mM KCl, 10mM Na2HPO4, 1.7 KH2PO4) + 1% phenylmethylsulphonyl fluoride (PMSF). The PBS was removed, and the cells were scraped in 5mL of fresh PBS with a cell scraper. The cells suspended in PBS were collected in a 50 mL tube and an additional 5 ml of PBS was added to the plate to recover the remaining cells. The cells were pelleted and the majority of supernatant removed. The pellet was resuspended in residual volume (approximately 1ml) and transferred to 1.5 mL tubes. The cells were pelleted again and all of the supernatant was removed. The pellet was resuspended in 200 μl

of nuclear lysis buffer (20 mM HEPES pH 7.9, 500mM NaCl, 20 mM EDTA, 1.5 mM $MgCl_2$, 20% glycerol, 0.1% Triton-X 100 + 1% PMSF) for each 10 cm plate used for the lysate. Cells were lysed by briefly sonicating at a low setting. The debris was pelleted and the supernatant collected.

Immunoblot analysis

Fifteen microlitres of each lysate were mixed with 15 ul of standard 2xSDS (sodium dodecyl sulfate) loading buffer and boiled at 95°C for 10min. The samples were size-separated on a 10% SDS-PAGE gel using the Protean 3 minigel system (BioRad). Protein from the gel was transferred to nitrocellulose membrane (Biorad) using a BioRad Protean 3 transfer apparatus in transfer buffer (20% methanol, 36mM Tris base, 275 mM glycine). The membrane was stained with Ponceau-S stain for 10 minutes to confirm proper transfer, then blocked with 5% milk powder in TBST (100mM Tris-Cl pH 7.5, 150 mM NaCl, 0.05 % Tween-20) for 30 min. Antibodies (mouse monoclonal α-Xpress-HRP or α-V5-HRP (Invitrogen)) were diluted 1:5000 in TBST+milk and were incubated with the blot for 16 hours at 4°C. The blot was then washed six times for five minutes each with TBST. Antibody detection was performed using the Supersignal chemiluminescent substrate (Pierce) and exposing the membrane to film (Fuji).

Co-immunoprecipitation

Seventy-five microlitres of each whole cell lysate were diluted with 425 ul of Immunoprecipitation (IP) buffer (250 mM NaCl, 10mM HEPES pH 7.9, 0.25% IGEPAL CA-630). The diluted lystaes were pre-cleared for two hours with 30ul of blocked protein G-sepharose beads. The protein G beads had been previously blocked with 1%BSA in PBS. The beads were removed by centrifugation and the supernatants were allowed to bind with the appropriate antibody (mouse monoclonal α-Xpress or α-V5) overnight at 4°C. Thirty microlitres of new blocked beads were added to the reaction and allowed to batch bind for one hour. The beads were pelleted by centrifugation at 1000 x g for five minutes and resuspended in IP buffer for a five minute batch wash. The washes were repeated five more times. Finally the

antibody/protein-complexes were eluted from the beads in standard 2x SDS loading buffer. SDS-PAGE and immunoblot analysis were performed as above. For increased sensitivity, the blot was incubated for one hour incubation with a GαM-HRP secondary antibody (1:5000) following the anti-Xpress primary antibody incubation.

7) Intracellular localization

Immunofluorescence

COS-7 cells were maintained as described above, but seeded at $2x10^5$ on coverslips in 6-well plates. Transfections were performed as above with a total of 500 nanograms of DNA used per well.

Media was removed from wells and the coverslips were washed briefly with PBS prior to fixing the cells in 4% paraformaldehyde in PBS for 10 min. The fixative was removed by three PBS washes. To make the cells permeable, the coverslips were exposed to three five minute changes of 0.1% Triton X-100 in PBS. The coverslips were then blocked for one hour in PBS 5% BSA, and rinsed briefly with PBS-1% BSA. The cells were exposed to a 1/500 dilution of the α-V5 primary antibody for one hour at room temperature. The coverslips were then washed with six changes of PBS-BSA for five minutes each. Following these washes, the cells were exposed to a 1/500 dilution of GαM-Cy3 secondary and Hoechst (50 μg/ml) for one hour, washed twice for five minutes in PBS-BSA and twice for five minutes in PBS. The coverslips were mounted in mounting media (9:1 glycerol to PBS, and 5 mM p-phenylenediamine) and sealed to slides with nail polish.

Co-Immunofluorescence (performed in collaboration with Matthew Lines)

In the interest of time, the pcDNA V5-EFEMP2$_{\Delta N36}$ construct was provided to Matthew Lines to perform a co-immunofluorescence experiment with a pCI derived construct encoding an N-terminally tagged HA-PITX2 fusion protein (created by Kathy Kozlowski). The transfections were performed as above, but using 250 nanograms of the EFEMP2 construct and 250 nanograms of the PITX2 constructs. The immunofluorescence was performed as above with anti-V5 mouse primary

antibody and anti-HA rabbit primary antibody being incubated on the slide simultaneously. Following six, five minute PBS-BSA washes, the secondary antibodies (goat-anti-mouse-Cy3 secondary and donkey-anti -rabbit -Cy2 secondary) were incubated on the slide simultaneously.

Microscopy and Imaging

The prepared slides were viewed using a Leica DMRE microscope with the 40x or 100x objective. Three filters separated the fluorescent signals: filter 31000 for Hoechst, 41001 for Cy2, and 31002 for Cy3. Photographs were taken with a QICAM 10-bit mono CCD camera. Image merges and alignments were done using Northern Elite imaging software.

8) Primer set design for mutational screens

The Primer 3 program was used to design intronic primer sets that span one or more EFEMP2 exons and their intron junctions. Primer 3 source code is available at http://frodo.wi.mit.edu/primer3/primer3_code.html.

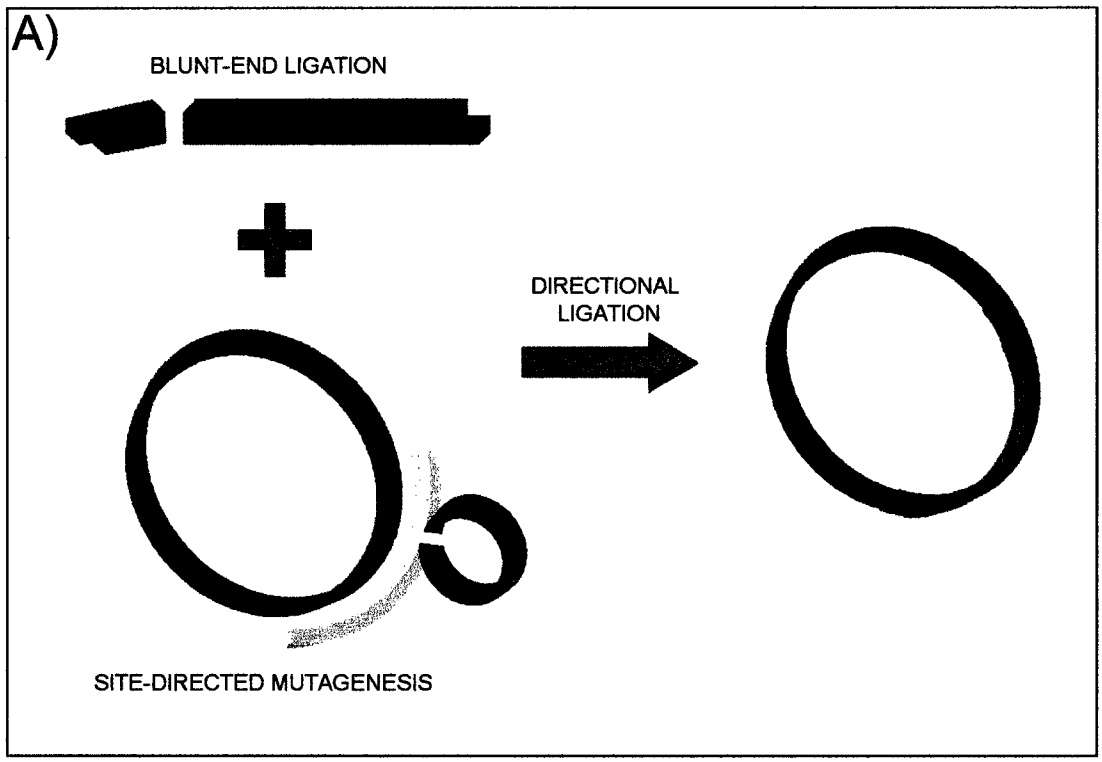

B)

attB1 cDNA Adapter

EcoRI Overhang

5′OH–AATTCGGGGGGACAAGTTTGTACAAAAAAGCAGGCTCG3′
3′ GCCCCCCTGTTCAAACATGTTTTTTCGTCCGAGCp5′

attB2/pMyr Mutagenesis Primers

5′CCGGGCCTCGAGGTCGACGGACCCAGCTTTCTTGTACAAAGTGGTCCCCTAATTGAATAATAAGC3′
3′GGCCCGGAGCTCCAGCTGCCTGGGTCGAAAGAACATGTTTCACCAGGGGATTAACTTATTATTCG5′

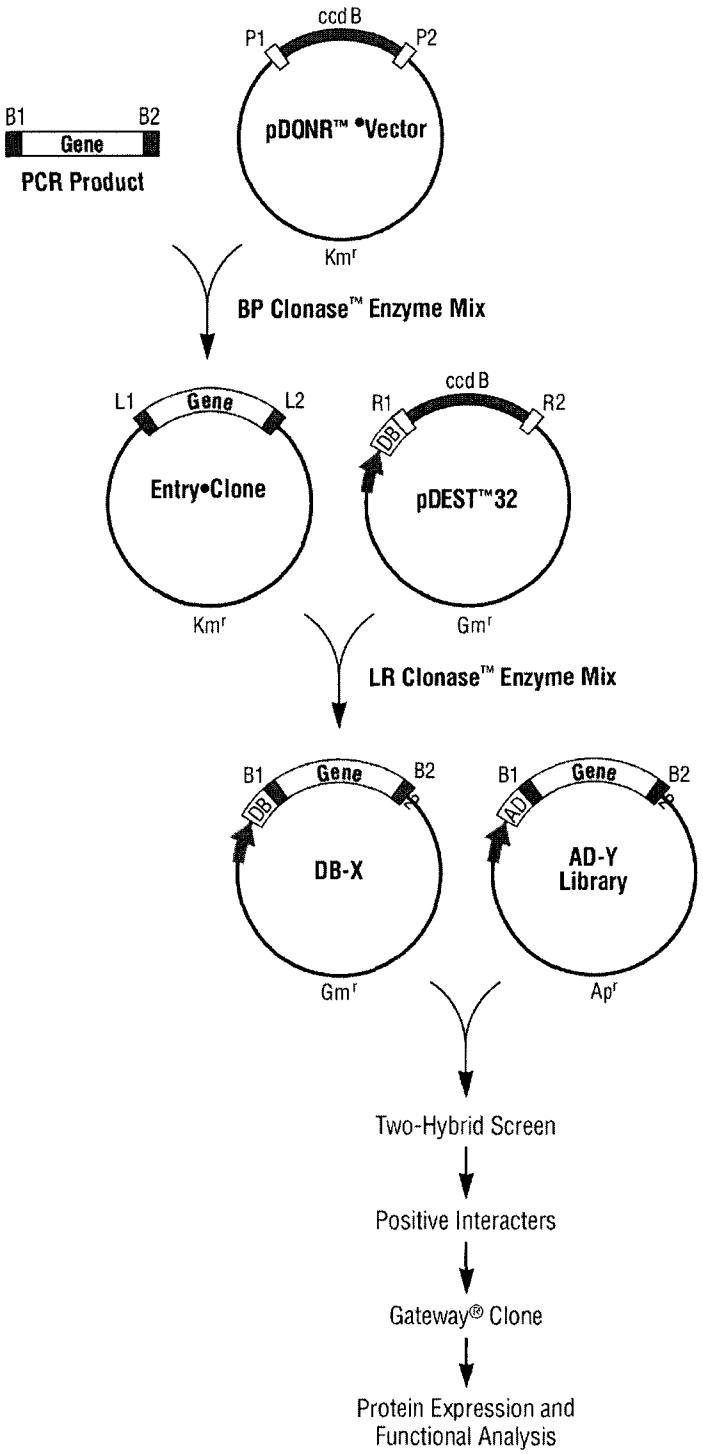

Table 2-1: Primer sequences - listed 5' to 3'

Sequencing:	
Myr 5' primer	act act agc agc tgt aat a
Myr 3' primer	cgt gaa tgt aag cgt gac at
pDEST-32 forward	ttg act gta tcg tcg agg
pDEST-32 reverse	ttg tac aag aaa gct ggg
pEXP-AD502 forward	cgg tcc gaa cct cat aac aac tc
pEXP-AD502 reverse	gta aat ttc tgg caa ggt aga c
T7 primer	taa tac gac tca cta tag gg
PCR:	
Full length PITX2 *att*B1 forward	
gggg aca agt ttg tac aaa aaa gca ggc tta atg gag acc aac tgc cgc	
Full length PITX2 *att*B2 reverse	
gggg ac cac ttt gta caa gaa agc tgg gta cac ggg ccg gtc cac tg	
Homeodomain PITX2 *att*B1 forward	
gggg aca agt ttg tac aaa aaa gca tac ccg tct aag aag aag cgg	
Homeodomain PITX2 *att*B2 reverse	
gggg ac cac ttt gta caa gaa agc tgg gtg ctc ggc ctg ctg gtt gcg	

Chapter Three: Results

CytoTrap library construction

The cDNA library created with porcine (*Sus scrofa*) anterior angle RNA consisted of approximately $2x10^3$ primary colony forming units (pcfu). Ten out of ten randomly picked library colonies contained cDNA inserts by restriction analysis. The sizes ranged from 200bp to 3.5 kb (data not shown). Three of these clones were sequenced and revealed identity to *Sus scrofa* expressed sequence tags (ESTs).

Because the major goal of the porcine library creation was to develop a modified system to be used with HTM RNA, the Gateway modifications were examined. The presence of both the *att*B1 and *att*B2 sites were confirmed by LICOR sequencing and their functionality was successfully tested by a BP recombination reaction and confirmed by restriction analysis.

A human fetal eye cDNA library was also created within this system in collaboration with James Friedman (former graduate student, Walter lab). The human fetal eye library contained a higher number of pcfu ($3.8x10^4$) than the porcine library. Both *PITX2* and *FOXC1* transcripts were detected in the fetal eye library by PCR of the cDNA library DNA extract. The human fetal eye cDNA library was test-screened using FOXC1 as the Y2H bait protein (Fred Berry personal communication). No FOXC1 interacting proteins were identified. Due do the low numbers of pcfu in the porcine and human fetal eye libraries and the negative results from the CytoTrap FOXC1 Y2H screen, these libraries were abandoned.

Commercial HTM cDNA library construction and initial analysis

Total RNA from a HTM primary cell culture was provided to us by our collaborator Dr. Jon R. Polansky. The presence of rRNA bands with a 28S to 18S ratio greater than 2:1 in the HTM total RNA indicates high quality and integrity (figure 3-1a). The HTM cDNA library was created with a commercially available service with guaranteed results (Invitrogen).

Approximately 10μg of poly-A enriched RNA was isolated from 100μg of total RNA (figure 3-1a). The poly-A enriched RNA sample was estimated to contain only 0.5-1 μg of mRNA (Pei-zhong Tang, Invitrogen, personal communication). This

mRNA was used as the starting material for the Invitrogen micro-quantity cDNA custom library creation service. A library containing $1x10^6$ pcfu has a greater than 99% probability of including at least one copy of every mRNA (Chanda 1995). With $2.1x10^6$ pcfu, the created HTM cDNA library likely represents the entire transcriptome of the HTM cells. The HTM cDNA library was constructed in the Gateway-compatible ProQuest Two-Hybrid System prey vector (pEXP-AD502, Invitrogen). The ProQuest system uses low copy CEN-based plasmids and three independent, GAL4 activated, reporter genes to help eliminate false positives (figure 3-2).

Approximately 1.7 mg of plasmid DNA was isolated from the Invitrogen library glycerol stocks. Restriction digestion of the library plasmid DNA revealed a range of cDNA insert sizes. The cDNAs present themselves as a smear between one and five kb (see figure 3-1b). There is an apparent difference between average insert size in this figure (approximately 1.5kb) and that reported on Invitrogen's library certificate of analysis (1.9 kb). This difference is most likely due to *Bsr*GI recognition sites within some cDNA inserts. Internal *Bsr*GI sites would allow the enzyme to cleave the inserts into multiple fragments.

PITX2 is known to be expressed in the HTM tissue (Tomarev et al. 2003) and in our HTM primary cell culture (Kathy Kozlowski, personal communication). PCR analysis confirms the presence of a full length PITX2 transcript in our library (figure 3-1c).

Bait protein self-activation titration

When screening a Y2H library, it is important to determine whether or not the bait fusion protein will self-activate the reporter genes in the absence of an interacting prey protein. The chemical 3-Aminotriazole (3AT) competitively inhibits the HIS3 gene product and can be used to titrate self activation of bait proteins. Both full-length and homeodomain (amino acids 33-104, inclusive) PITX2 bait constructs were created in anticipation that a full length PITX2 protein would contain transactivation domains with untitratable self-activation ability (>100mM 3AT). Both the full length PITX2 and PITX2 homeodomain bait proteins were found not to self activate at

25mM 3AT (figure 3-3). I was able to use the full length PITX2 bait construct to screen the HTM library by supplementing the selection media with 25 mM 3AT.

PITX2 dimerization

In parallel with the library screen, a known PITX2 protein-protein interaction was tested directly within the Y2H system. The ability of PITX2 to form homodimers is an Axenfeld-Rieger Syndrome related protein-protein interaction ((Saadi et al. 2003) and Matthew Lines personal communication). A full length PITX2 prey construct was created by shuttling the PITX2 bait insert into the prey vector (pDEST-22, Invitrogen). The PITX2 prey protein does not self activate at 25mM 3AT. PITX2 bait and PITX2 prey co-transformants did not demonstrate an interaction phenotype in this Y2H system. These results were later reproduced by Lijia Huang using the same method (personal communication).

Yeast two-hybrid library screen

The HTM cDNA library was screened twice with full length PITX2 as bait. In the first screen, $5x10^4$ co-transformants were screened. Fourteen small (< 1mm) and two large ($\geq$ 2mm) colonies were isolated. In the second screen 10 small and 13 large colonies were isolated from $2.56x10^5$ co-transformants screened (table 3-1). Large colonies first appear on media lacking histidine three-four days after plating, while small colonies only became apparent after six or seven days.

Taken together, approximately 300,000 co-transformants were screened, resulting in 39 putative interaction colonies (table 3-1). Of these 39, 16 displayed a HIS+ βgal + URA- 5FOA- interaction phenotype. An 5FOA- scoring can mean an absence of growth, or growth inhibition on media supplemented with 5-fluoroorotic acid. Figure 3-4 displays a colony representative of this phenotype. With only two exceptions (2P071 and 2P112), the colonies displaying an interaction phenotype were the large colonies. The 2P071 small colony displayed a putative interaction phenotype (HIS+ βgal - URA- 5FOA-), was discovered to be a false positive. The identity of 2P071 was determined to be an out of frame cDNA for the Mannose 6 Phosphate Receptor Binding Protein (M6PRBP). The 2P071 prey protein produces a

very short truncated novel peptide (20 AA) that does not show similarity to any known proteins by BLASTp analysis. The putative interaction phenotype of 2P071 is probably a result of inconsistent replica plating or replica cleaning, but may be due to a host cell mutation or bait/prey construct self-activation mutations. 2P112 was a large colony that initially grew on media lacking histidine, but displayed a non-interaction phenotype (HIS- βgal - URA- 5FOA+). 2P112 represents a false positive that was eliminated from further characterization due to the inactivation of the three independent reporter genes.

The two-hybrid plasmids were recovered from the putative interacting colonies (figure 3-5) and the prey plasmids were sequenced (table 3-2). Fourteen prey constructs contained cDNAs with identity to the EGF-containing fibulin-like extracellular matrix protein 2 gene (*EFEMP2*) by BLASTn analysis. No cDNA containing prey plasmids were recovered for the 2P061 colony from three independent bacterial colonies.

Of the EFEMP2 cDNAs recovered, there were nine different clone lengths ranging from 309 to 407 amino acids of EFEMP2's putative 443 amino acid open reading frame (ORF). No EFEMP2 clones were isolated during an equivalent, parallel HTM library screen of 300,000 co-transformants with FOXC1 as bait (Lijia Huang, personal communication). This implies that EFEMP2 interactions are specific to the PITX2 protein.

EFEMP2/PITX2 interaction confirmation in yeast

To confirm the EFEMP2/PITX2 interaction within the ProQuest system and eliminate the possibility of a host cell or construct self-activation mutation, the longest (2P152 now called EFEMP2$_{\Delta N36}$) and shortest (2P141 now called EFEMP2$_{\Delta N134}$) EFEMP2 prey constructs were re-co-transformed with the original full length PITX2 bait construct and an empty bait vector. At this point I also tested the ability of the EFEMP2$_{\Delta N36}$ or EFEMP2$_{\Delta N134}$ clones to interact with a PITX2 homeodomain (PITX2-HD) bait protein and a full length FOXC1 bait protein (construct supplied by Lijia Huang). Initial protein-protein interaction domain mapping was provided by testing the EFEMP2 $_{\Delta N36}$/PITX2-HD interaction. The

EFEMP2 $_{\Delta N36}$/FOXC1 acts as a negative control that demonstrates the specificity of the PITX2/EFEMP2 interaction showing that EFEMP2 does not interact with all transcription factors or GAL4-fusion proteins.

Both EFEMP2 clones recapitulated the original interaction phenotype with full length PITX2 (figure 3-6). Neither EFEMP2$_{\Delta N36}$ nor EFEMP2$_{\Delta N134}$ demonstrated an interaction with the empty bait vector, PITX2 homeodomain or full length FOXC1 in this system. The negative result of the X-gal assay shown here is representative of the HIS, URA, and 5FOA non-interaction phenotypes.

Confirmation of the PITX2/EFEMP2 interaction in a mammalian system

Once the PITX2/EFEMP2 interaction was confirmed within the yeast system, the next step was to test the interaction in a second system. A bidirectional co-immunoprecipitation (co-IP) experiment was performed by expressing tagged versions of PITX2 and EFEMP2 in COS-7 cells. I created a mammalian expression vector construct encoding an N-terminally tagged V5-EFEMP2$_{\Delta N36}$ protein by shuttling the cDNA insert from the Y2H prey vector to pcDNA3.1/nV5-DEST using Gateway technology. I then transiently expressed this EFEMP2$_{\Delta N36}$ fusion protein and an N-terminally tagged Xpress PITX2 in COS-7 cells. Both fusion proteins were detected by immunoblot analysis in the COS-7 cell lysates, but the V5-EFEMP2$_{\Delta N36}$ band is approximately 5 kDa larger than would be expected for the 50 kDa V5-EFEMP2$_{\Delta N36}$ fusion protein (figure 3-7). This decreased EFEMP2$_{\Delta N36}$ mobility corresponds to the decreased mobility demonstrated with full length EFEMP2 and is most likely due to post-translational modifications (Giltay et al. 1999; Gallagher et al. 2001).

To test if PITX2 and EFEMP2 proteins interact in a mammalian system, co-IP experiments were performed with α-V5 and α-Xp antibodies. If PITX2 and EFEMP2 interact, the proteins will be immunoprecipitated as a complex when either one is precipitated with a specific antibody. EFEMP2$_{\Delta N36}$ was co-immunoprecipitated with PITX2. PITX2 was co-immunoprecipitated with EFEMP2$_{\Delta N36}$ in the reciprocal experiment (figure 3-8). Neither fusion protein was immunoprecipitated in the absence of their respective interacting partner (empty vectors controls). The inability

of peptides encoded by the empty vector to co-immunoprecipitate PITX2 or EFEMP2 indicates that the PITX2/EFEMP2 interaction is occurring through a specific protein-protein interaction and not with the N-terminal Xpress or V5 tags.

Intracellular localization

Immunofluorescence experiments were performed to examine whether the co-IP EFEMP2/PITX2 interaction detected in COS-7 lysates was also occuring within live cells. Cells expressing V5-EFEMP2$_{\Delta N36}$ display both nuclear and cytoplasmic fluorescent staining (figure 3-9). As compared to a soluble cytoplasmic localization control (V5-LacZ), V5- EFEMP2$_{\Delta N36}$'s cytoplasmic staining appears more punctate. The EFEMP2$_{\Delta N36}$ transfected cells displayed varied subnuclear localization (figure 3-9). The transfected cells have variously sized nuclear foci that are excluded from the regions of highest Hoechst staining. High levels of Hoechst stain are areas of concentrated DNA and represent constitutive heterochromatin. The larger EFEMP2$_{\Delta N36}$ nuclear foci appear to localize where no DNA stain is visible. These areas represent extrachromatic or possibly highly decondensed euchromatic regions. COS-7 cells transfected with the empty V5 vector did not show fluorescence (data not shown).

When COS-7 cells were co-transfected with PITX2 and EFEMP2$_{\Delta N36}$ expressing constructs, 50% of transfected cells expressed PITX2 only, 25% expressed EFEMP2$_{\Delta N36}$ only and 25% expressed both proteins. Cells expressing HA-PITX2 display nuclear localization consistent with previous studies (Matthew Lines, personal communication) (figure 3-10a). Cells expressing both exogenous PITX2 and EFEMP2$_{\Delta N36}$ display wild-type PITX2 intracellular localization, but the EFEMP2$_{\Delta N36}$ protein is now more strongly localized to the nucleus (figure 3-10a). In particular, the presence of recombinant PITX2 alters the subnuclear localization of EFEMP2$_{\Delta N36}$ to resemble PITX2 subnuclear localization (figure 3-10b).

PITX2 and EFEMP2 *in silico* tissue expression profile comparison

PITX2 and *EFEMP2* virtual Northern blots show an overlap of expression in many normal human adult tissues (table 3-3). *PITX2* and *EFEMP2* are co-expressed

in 11/13 *PITX2* expressing tissue groups and 11/23 *EFEMP2* expressing tissue groups. *PITX2* and *EFEMP2* co-expression in the eye is of particular interest to this study. Gene expression in uninformative tissue groupings such as 'unclassified', 'other', and 'mixed' are not shown.

Primers designed for candidate disease patient mutational screening

Primer sets were designed to do mutational screening of the *EFEMP2* putative coding region and intron/exon boundaries (figure 3-11). These primer sets are currently being used for screening the DNA of patients with candidate ocular diseases (Farideh Mirzayans and Dion Pasichnyk personal communication).

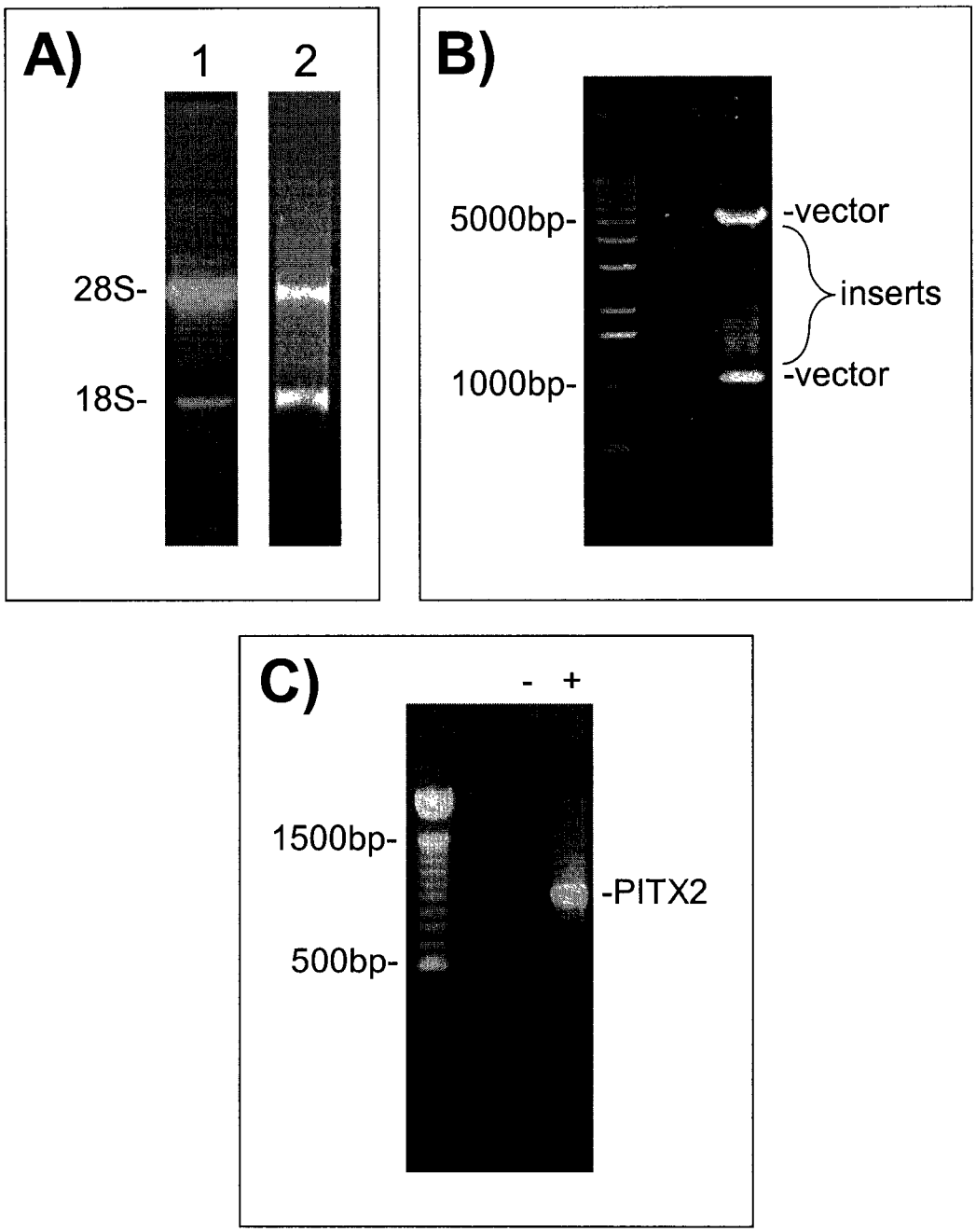

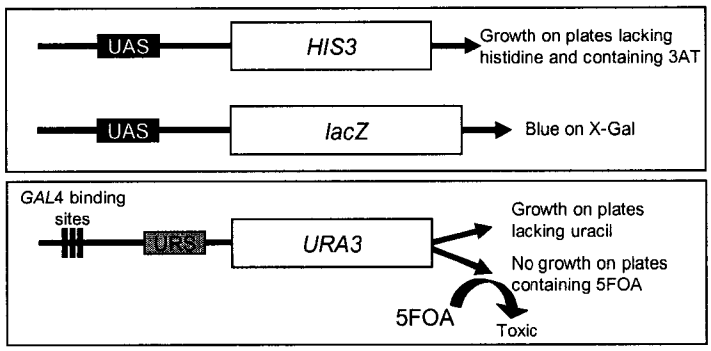

Reporter Phenotype

Protein-Protein Interaction

	HIS	X-Gal	URA	5FOA
No Interaction	-	White	-	+
Weak Interaction	+	Blue	-	+
Moderate Interaction	+	Blue	-	-
Strong Interaction	+	Blue	+	-

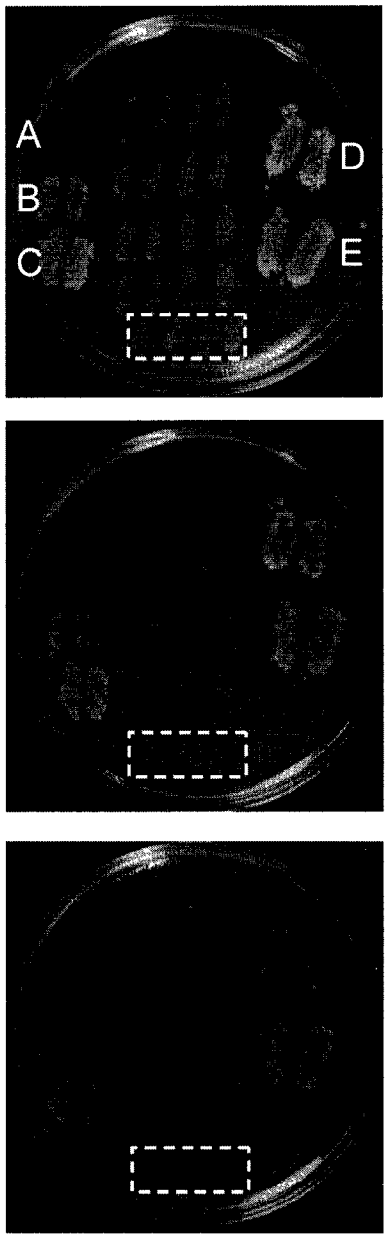

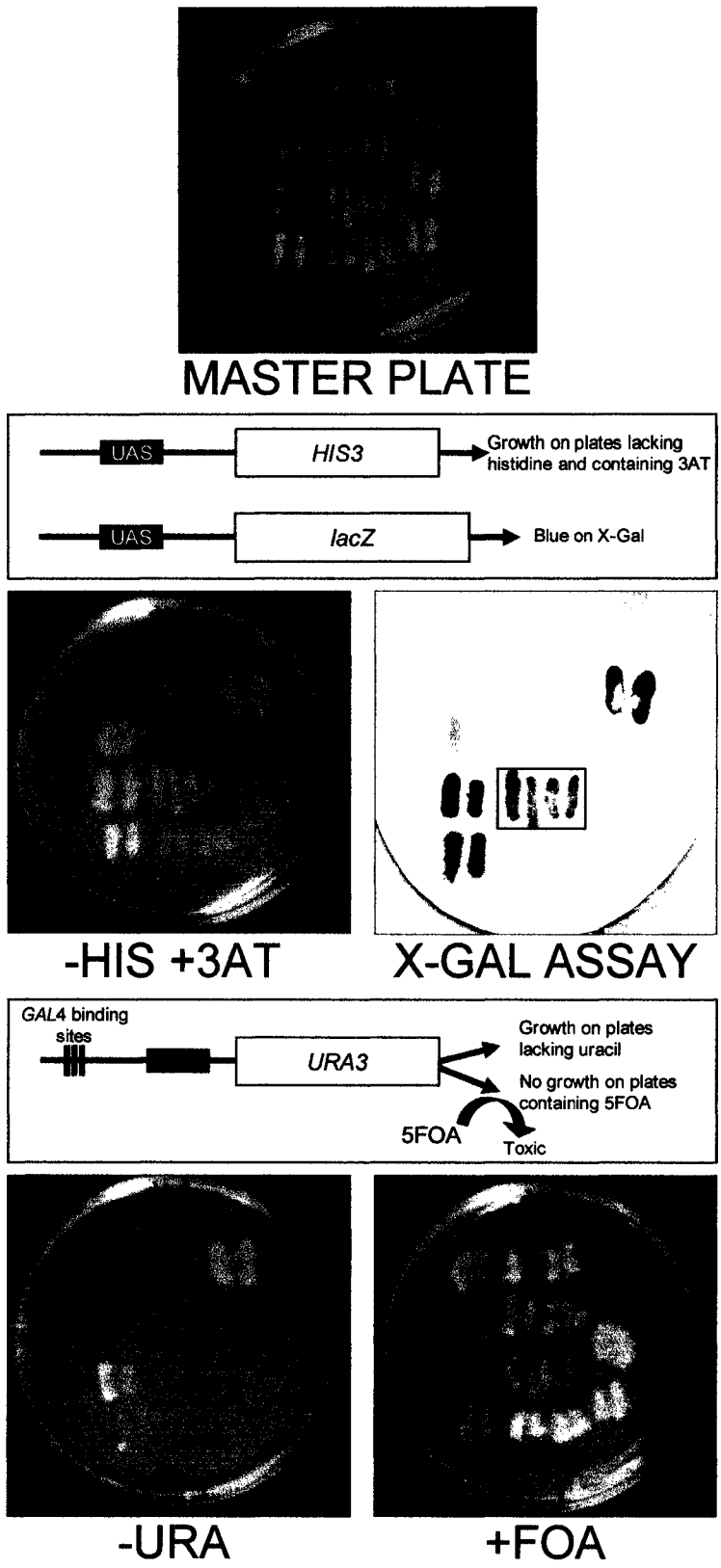

Table 3-1: Yeast Colony Reporter Gene Phenotypes

COLONY #	COLONY SIZE	HIS	X-GAL ASSAY	URA	FOA	INTERACTION PHENOTYPE
P011	s	-	-	-	+	N
P012	s	-	-	-	+	N
P021	l	+	+	-	inhibited	
P031	s	-	-	-	+	N
P032	s	-	-	-	+	N
P033	s	-	-	-	+	N
P051	s	-	-	-	+	N
P061	s	-	-	-	+	N
P062	s	-	-	-	+	N
P091	s	-	-	-	+	N
P092	s	-	-	-	+	N
P094	s	-	-	-	+	N
P095	s	-	-	-	+	N
P101	l	+	+	-	inhibited	
P161	s	-	-	-	+	N
P162	s	-	-	-	+	N
2P031	l	+	+	-	-	
2P041	l	+	+	-	inhibited	
2P042	s	-	-	-	+	N
2P051	s	-	-	-	+	N
2P061	l	+	+	-	inhibited	
2P062	l	+	+	-	inhibited	
2P063	s	-	-	-	+	N
2P064	l	+	+	-	-	
2P071	s	slight	-	-	inhibited	
2P091	s	-	-	-	+	N
2P101	l	+	+	-	inhibited	
2P102	s	-	-	-	+	N
2P111	l	+	+	-	-	
2P112	l	-	-	-	+	N
2P113	s	-	-	-	+	N
2P121	s	-	-	-	+	N
2P131	l	+	+	-	+	
2P141	l	+	+	-	+	
2P142	s	-	-	-	+	N
2P151	l	+	+	-	-	
2P152	l	+	+	-	inhibited	
2P161	l	+	+	-	inhibited	
2P162	l	+	+	-	inhibited	
					TOTAL:	

s-small + = growth or blue with X-gal Y=yes
l-large - = no growth or white X-gal N=no

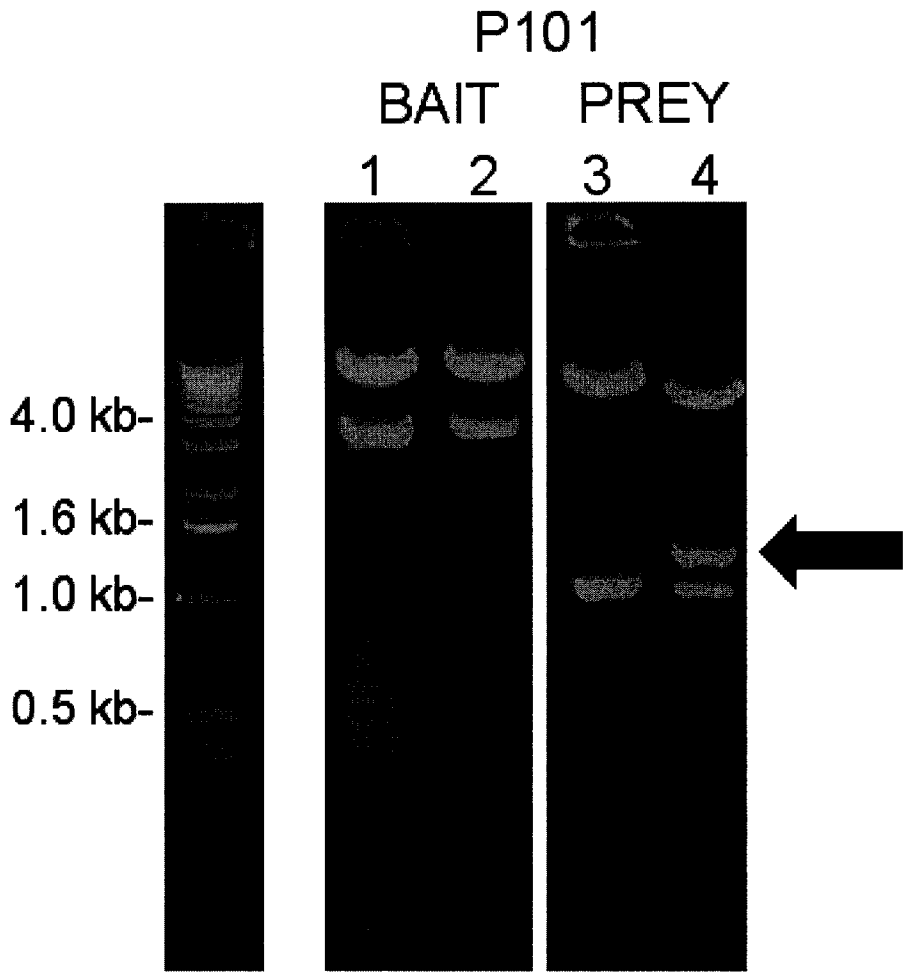

Table 3-2: cDNA Identity of PITX2 Interacting Prey Constructs

COLONY #	Sequence Identity	Length of novel ORF(AA)
P021	EFEMP2	319
P101	EFEMP2	347
2P031	EFEMP2	347
2P041	EFEMP2	369
2P061	empty vector*	N/A
2P062	EFEMP2	364
2P064	EFEMP2	355
2P071	M6PRBP1	not in frame
2P101	EFEMP2	355
2P111	EFEMP2	355
2P131	EFEMP2	369
2P141	EFEMP2	309
2P151	EFEMP2	384
2P152	EFEMP2	407
2P161	EFEMP2	388
2P162	EFEMP2	347

* probable mixed population

- Shortest and longest EFEMP2 clones selected for additional analyses

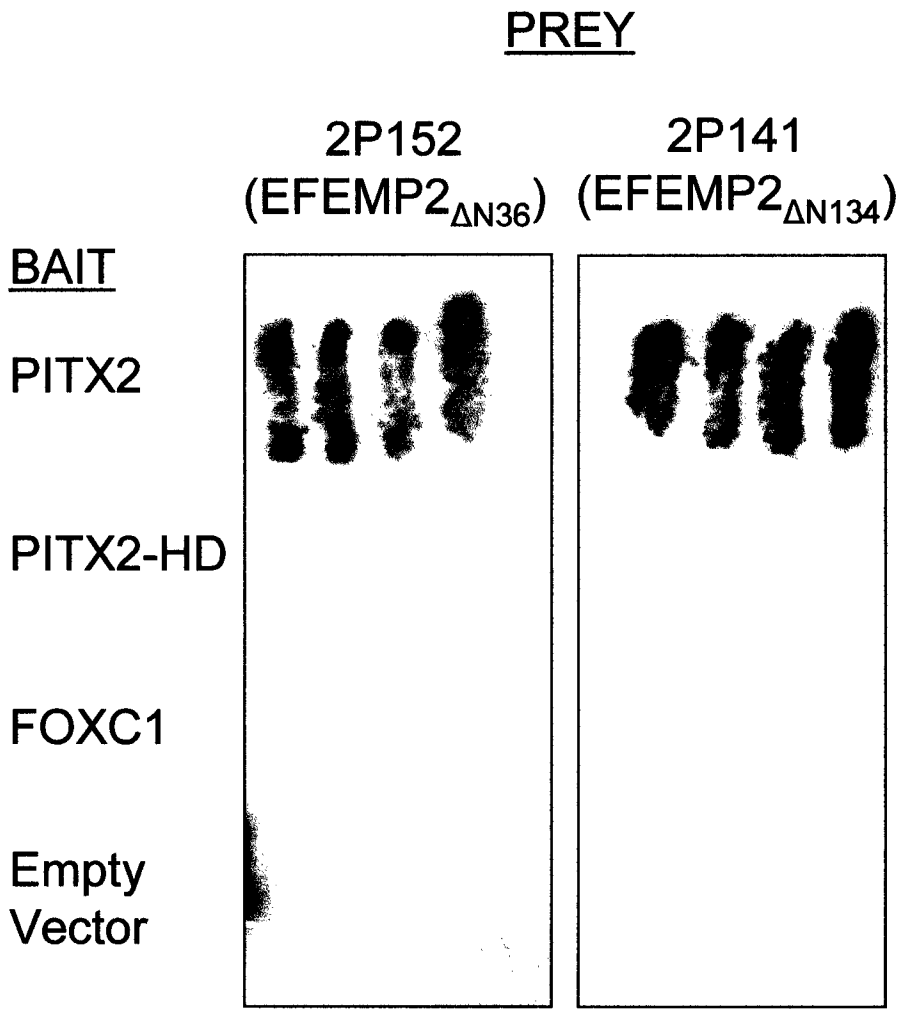

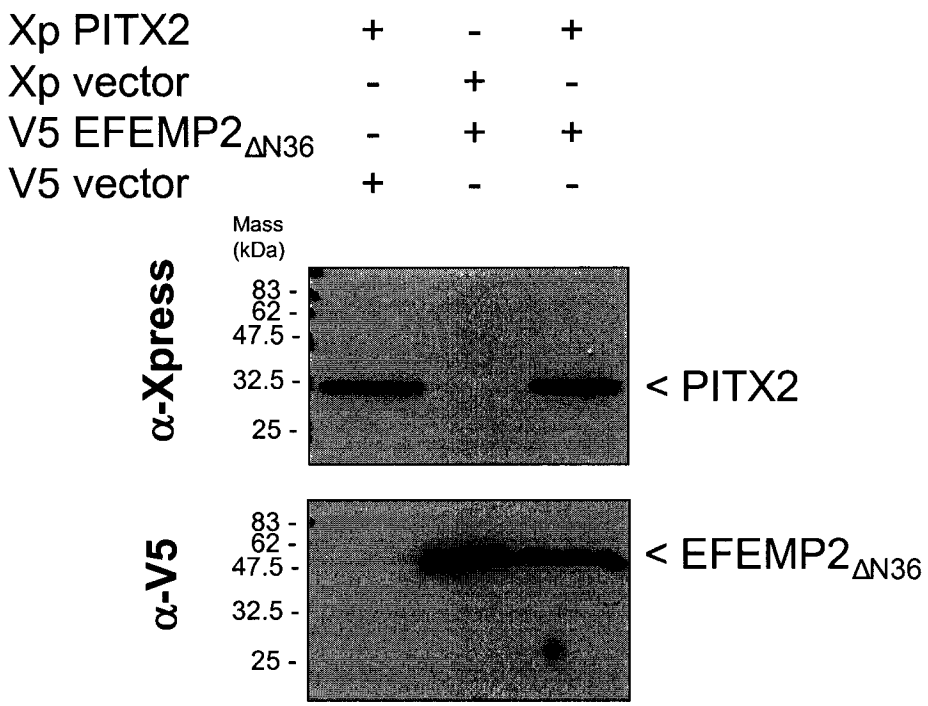

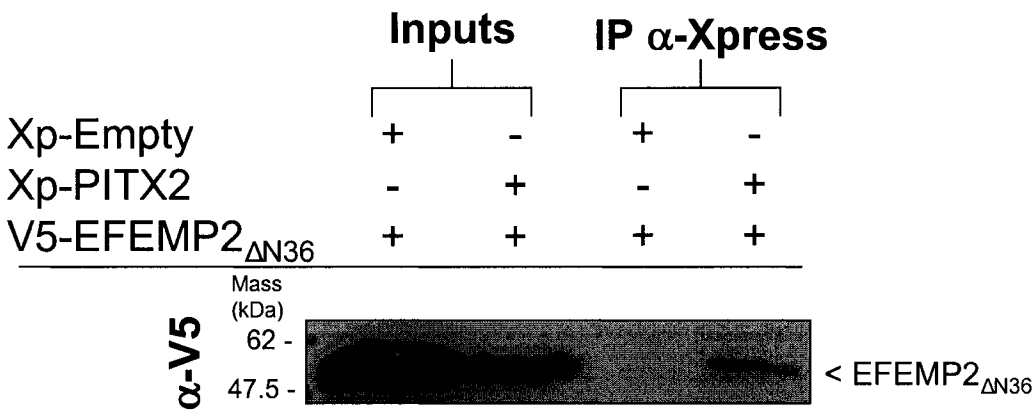

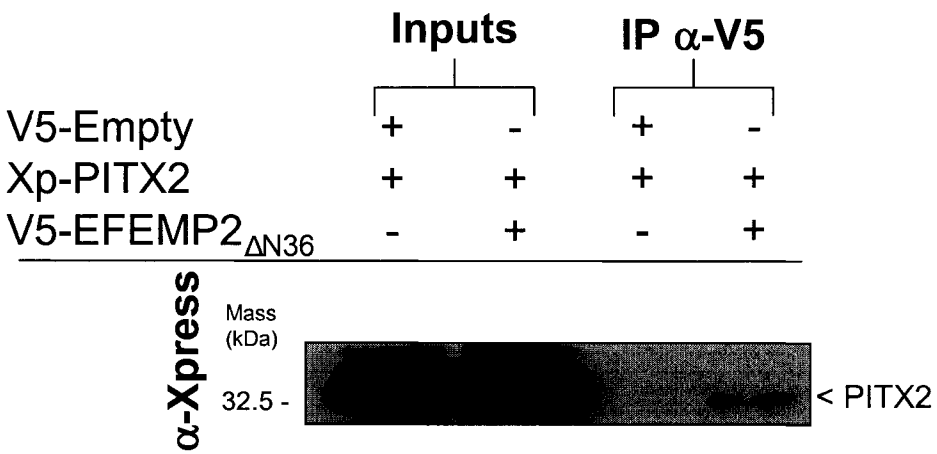

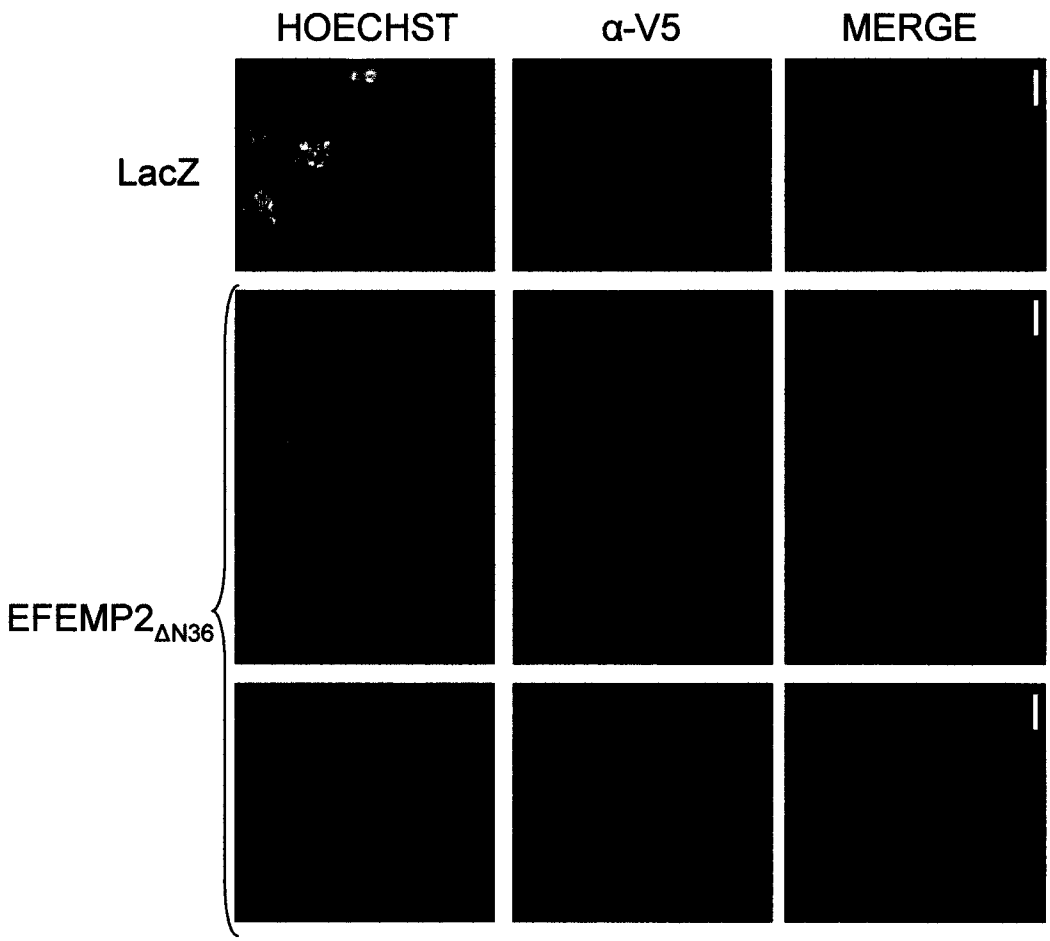

A)

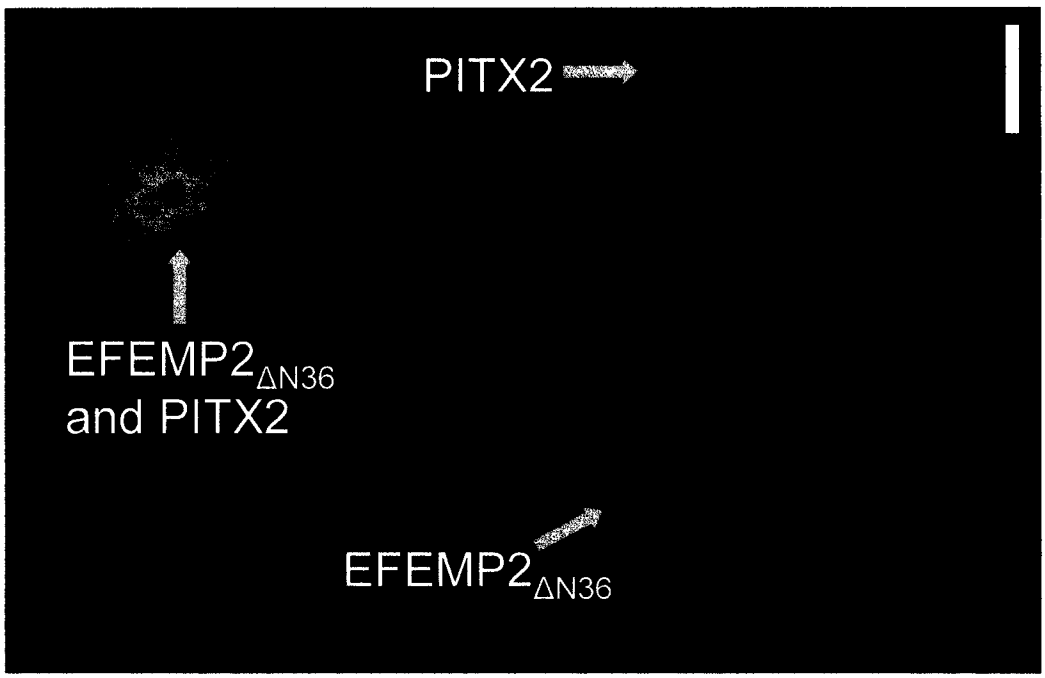

B)

HOECHST α-V5 α-HA MERGE

Table 3-3: PITX2 and EFEMP2 human normalized virtual Northern blots

PITX2

Tissue Type	Percentage of Normalized Abundance
Tongue	41.15
Placenta	15.10
Eye	14.78
Cervix	9.37
Muscle	3.39
Heart	2.89
Uterus	2.39
Bone	2.00
Colon	1.25
Testis	0.95
Lung	0.91
Kidney	0.90
Liver	0.88

EFEMP2

Tissue Type	Percentage of Normalized Abundance
Thymus	14.61
Bone	11.39
Heart	8.85
Placenta	7.24
Brain	4.22
Eye	3.95
Kidney	3.15
Prostate	2.79
Ovary	2.51
Uterus	2.45
PNS	2.14
Pancreas	1.99
Blood	1.95
Mamm Gland	1.75
Colon	1.64
Lung	1.59
Bone Marrow	1.53
Skin	1.50
Cervix	1.37
Muscle	0.99
Stomach	0.63
Testis	0.42
Lymph Node	0.39

- Tissues that express both PITX2 and EFEMP2

PNS – Peripheral Nervous System
Mamm Gland – Mammary Gland

Exon(s)	Forward Primer (5'-3')	Reverse Primer (5'-3')
1	ctcaggaatccgccgaag	ggcctctgtgggcgctac
2,3	ccggtacagggagttgagg	agctggcctctgtgtagcag
4	gctggggccacacatctc	gggaggaacatgaggtctgag
5	agaggttaggggtgcctttc	gtctgatgacggagggtgag
6,7	cctcggacacaggattatgg	ggagaactgtgtggcaggag
8,9	ttgtctcatccccctctgtc	tgattcccatcatccctcag
10	gggtagaagggtccttttgg	ccgagtgcttcgttagaattg
11,12	gccagggctgttcctctg	gagtgcagagggctcattg

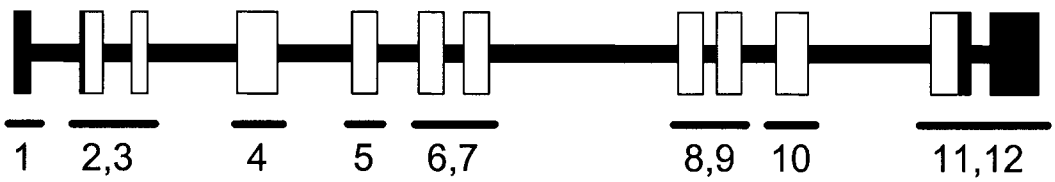

Chapter Four: Discussion

EFEMP2 is a PITX2 interacting protein

The major finding of this study is the identification of a novel PITX2 protein-protein interaction. When identifying a protein interaction, there are several criteria that must be met. In this study, I have fulfilled these major criteria and demonstrated that EFEMP2 is a PITX2 interacting protein. In brief, I have detected the protein-protein interaction within one system (yeast two-hybrid: an *in vivo* genetic system) and reassessed it within that system (figures 3-4 and 3-6). I then successfully confirmed the interaction within a second system (co-immunoprecipitation: an *in vitro* biochemical system) and in a reciprocal experiment within that system (figure 3-8).

Clones encoding EFEMP2 prey proteins of varying lengths were identified as PITX2 interactors from the Y2H library screen. Even prior to further interaction confirmation experiments, identification of multiple EFEMP2 clones was evidence that the PITX2/EFEMP2 interaction is genuine within the Y2H system and not just an artifact of a specific prey construct.

Through data-mining, I have shown both a temporal and spatial expression overlap of these two proteins. The normalized virtual Northern blots of PITX2 and EFEMP2 show a high degree of tissue expression overlap (table 3-3). As more specific evidence for *PITX2* and *EFEMP2* being expressed in the same tissues, the cDNA for these genes can be found within the same cDNA libraries: our HTM cDNA library, an infant HTM cell culture library (Wirtz et al. 2002), and a NEI Bank human optic nerve library. These tissues are extremely important in glaucoma pathogenesis. Co-expression of *PITX2* and *EFEMP2* in the same human tissues provides evidence that the proteins could interact in a biologically relevant manner.

Initial evidence for a developmental expression overlap is indicated by expression of both genes in human fetal tissues. Both *PITX2* and *EFEMP2* are expressed in fetal tissues and notably in the fetal eye (EST data, UniGENE). *Efemp2* is expressed at least as early as day seven and up to birth during mouse development (Gallagher et al. 1999). *Pitx2* shows expression in the developing mouse eye at days 10.5 and on (Hjalt et al. 2000). Common expression in fetal tissues provides

evidence that a PITX2/EFEMP2 interaction can potentially occur during development as well.

Further evidence for a physical interaction between EFEMP2/PITX2 is their expression overlap at the subcellular level demonstrated by intracellular co-localization (figure 3-10b). The PITX2/EFEMP2$_{\Delta N36}$ co-immunofluorescence results demonstrate that the PITX2/EFEMP2$_{\Delta N36}$ interaction is occurring within mammalian cell nuclei. PITX2 also induces EFEMP2$_{\Delta N36}$ nuclear translocation *in vivo*. This translocation is potentially accomplished through direct protein-protein binding and EFEMP2 relocation to the nucleus as a PITX2/EFEMP2 complex. This piggy-back model is similar to what occurs with the transcription factors Scalloped and Vestigal in Drosophila (Srivastava et al. 2002). Inside the nucleus, PITX2 alters the subnuclear localization of EFEMP2$_{\Delta N36}$ to a wild-type PITX2 pattern. The PITX2 subnuclear localization has been shown to be excluded from regions of transcriptional inactivity (Matthew Lines personal communication). This is consistent with PITX2 being involved in transcriptional activation. Therefore, the PITX2/EFEMP2$_{\Delta N36}$ complex is localized to areas of potential transcriptional activity and may be directly involved in transcriptional regulation.

All of the data I have outlined is consistent with PITX2 and EFEMP2 interacting *in vivo*. As *de facto* evidence of the interaction occurring in a biologically relevant context, the next step would be to visualize endogenous proteins *in vivo* in the same cells at the same time. This would require high-quality antibodies specific to the proteins and actual human tissue samples to do immunohistochemistry experiments. Nevertheless, my Y2H screen of the HTM cDNA library has identified a PITX2/EFEMP2 interaction as a novel protein-protein interaction.

EFEMP2 belongs to the fibulin family of proteins

The PITX2 interacting protein that I have identified (EFEMP2) is also named fibulin-4 (Giltay et al. 1999) and belongs to the fibulin family of proteins (Argraves et al. 2003; Timpl et al. 2003; Chu and Tsuda 2004). The fibulin name is derived from the latin word *fibul* which means clasps or buckles (Argraves et al. 1989). Fibulins are members of the epidermal growth factor (EGF) superfamily that includes EGF,

fibrillin proteins, Notch, amphiregulin, and hemicentin. There are five genes in the fibulin family, divided into two subgroups (figure 5-1). Fibulin-1 and fibulin-2 make up one group and contain N-terminal analphylatoxin domains. The fibulin-3, fibulin-4 (EFEMP2) and fibulin-5 subgroup are smaller proteins, do not contain analpylatoxin domains, and also differ from fibulin 1 and 2 in their gene structure.

Fibulin proteins contain epidermal growth factor (EGF) domains that span 35-40 amino acids and have a conserved spacing of six cysteine residues (Carpenter and Cohen 1990). These cysteine residues promote folding into β-sheet confirmations through disulfide bonds. Disulfide bond formations have been demonstrated in fibulins 3 and 4 by a electrophoretic mobility shift of the proteins treated in reducing versus non-reducing conditions (Giltay et al. 1999).

A subsection of EGF domains bind calcium (cbEGF domains). The cbEGF domains are identified by a consensus of negatively charged amino acid residues N-terminal to the first cysteine of the EGF domain. These cbEGF domains are thought to be involved in both intramolecular and intermolecular protein interactions (Rao et al. 1995). In fact, the presence of these specific EGF domains in fibulin proteins implies that fibulins interact with other proteins (Lecka-Czernik et al. 1995). Several fibulin protein-protein interactions have already been experimentally identified (table 4-1). Of these fibulin interactions, some are mediated by calcium ions (Timpl et al. 2003).

EGF and cbEGF domains are generally found in extracellular proteins, but there are examples of EGF containing intracellular proteins. Examples of intracellular containing EGF proteins include cyclooxygenases and peroxidases (Toh 1989; Toh et al. 1992) as well as amphiregulin (Modrell et al. 1992).

Fibulin proteins are involved in ocular function

There is evidence establishing roles for fibulin proteins in the eye. A mutation in the EFEMP1 (fibulin-3) gene has been determined to cause the allelic retinopathies: Doyne honeycomb retinal dystrophy and Malattia Leventinese (Stone et al. 1999). Recently, sequence variations in Fibulin 5 have been related to a leading cause of blindness, age related macular degeneration (ARMD), (Stone et al. 2004).

These studies demonstrate an important role for fibulin proteins within the eye and for vision. As a fibulin protein, EFEMP2 may also play a role within the eye.

EFEMP2 is a protein of unknown function

Fibulin-4 (EFEMP2) is the least characterized member of the fibulin family. It has received little experimental attention to date, but the results of the few EFEMP2 studies provide initial characterization of the *EFEMP2* gene and EFEMP2 protein.

The EFEMP2 hamster ortholog (H411) was discovered by differential expression in a bacterially induced inflammatory response study (Heine et al. 1999). The mouse cDNA (MPBP1) was identified in a yeast two hybrid screen of a mouse embryo library using mutant p53 as bait (Gallagher et al. 1999). Human EFEMP2/Fibulin-4 was independently cloned by two groups, hence the two different names (Giltay et al. 1999; Katsanis et al. 2000). The human *EFEMP2* locus has been mapped to 11q13 by two independent studies. It was radiation hybrid mapped to 11q then fine mapped to 11q13 (Katsanis et al. 2000) and fluorescence *in situ* hybridization (FISH) (Gallagher et al. 2001). The 11q13 area is a gene-rich with a density as high as one gene every 15 kb (Katsanis et al. 2000).

As discussed earlier, *EFEMP2* is expressed throughout the human body (table 3-3). The virtual Northern blot data agree with the available *EFEMP2* experimental expression analysis. EFEMP2 has been shown to be expressed in human heart, brain, placenta, lung, skeletal-muscle, kidney, pancreas, and liver (Giltay et al. 1999; Katsanis et al. 2000; Gallagher et al. 2001), as well as spleen, prostate, testis, ovary, intestine, colon, leucocytes,(Gallagher et al. 2001) by Northern blot analysis. Katsanis et al. also demonstrated *EFEMP2* expression at RT-PCR levels in fetal brain, kidney, heart retina, adult retina but not fetal lung (Katsanis et al. 2000). *EFEMP2* expressed sequence tags (ESTs) have been identified in trabecular meshwork, iris, normal pigmented retinal epithelium, optic nerve, eye, fetal eyes, lens, eye anterior segment, retina, choroids, foveal and macular retina libraries (UniGene EST data).

EFEMP2 has a modified cbEGF domain near the N-terminus of the protein. This domain is classified as a modified domain because it contains an insertion of

amino acids between the forth and fifth EGF conserved cysteines. This insertion is not predicted to interfere with disulfide bond formation (Giltay et al. 1999). EFEMP2 contains five tandem cbEGF domains C-terminal to the modified cbEGF domain. (Katsanis et al. 2000). At the C-terminus of the EFEMP2 protein there is a region conserved between fibulin proteins designated as the C-terminal fibulin (FC) domain. EFEMP2's FC domain shares higher similarity to fibulin-3 and 5 than fibulin-1 and 2 (Chu and Tsuda 2004). The domain structure of EFEMP2 agrees with the fibulin subgroup division that fibulins 3-5 are more closely related to each other than to fibulins 1-2 (figure 4-1).

In addition to the cysteine di-sulfide bonds inherent to EGF domains, EFEMP2 may also be modified in other ways. There is a predicted signal peptide encoded by amino acids one through 27. If functional, the signal peptide would be cleaved co-translationally. There are also possible sites for addition of N-glycosylation type sugar residues to EFEMP2. The 443 amino acid protein displays an electrophoretic mobility of 54 kDa, when it is predicted to be only 49.4 kDa. This mobility is increased to 51 kDa after removing N-glycosylations (Gallagher et al. 2001), suggesting there may still be another type of protein modification.

No biological role or function has been established for EFEMP2. The initial characterization of *EFEMP2* and its protein product is limited. The identification of EFEMP2 as a PITX2 interacting protein has added to EFEMP2's characterization.

PITX2/EFEMP2$_{\Delta N36}$ interaction models

As a fibulin protein, EFEMP2 is generally thought of as a secreted protein. This presents an apparent paradox in my conclusion that a protein known to be intracellular and nuclear (PITX2) is interacting with an extracellular protein. However, there is substantial evidence that *EFEMP2* encodes an intracellular protein or at least a protein that has an intracellular form.

There are at least five, and as many as eight, different sized *EFEMP2* transcripts identified on human northern blots. Giltay *et al.* identified 1.5 and 1.9 kb transcripts (Giltay et al. 1999) using a randomly primed probe from an EFEMP2 cDNA. A second study demonstrated a 2.0 kb transcript in most tissues, an additional

2.2 kb transcript in placenta, and 4.0 and 8.0 kb transcripts in brain using a probe derived from the 3' UTR of EFEMP2 (Katsanis et al. 2000). Katsanis *et al.* also performed Southern blot analysis with the same EFEMP2 probe. They detected a single 5.4 kb band suggesting that the multiple bands on the Northern blots are probably mRNA isoforms and not other family members only expressed in placenta or brain. A third research group detected 1.5 and 1.8 kb EFEMP2 transcripts in multiple tissues (Gallagher et al. 2001). The 1.8, 1.9 and 2.0 kb bands identified by different groups may all represent the same sized transcript, but it is important to note that a size difference as little as 100bp is important because nine of the *EFEMP2* exons are 127 bp or less in size. The tissue-specific splicing activity seen here can result in tissue-specific protein forms.

These different splice variants may encode alternate EFEMP2 protein forms from an alternate 3' or 5' translation start site. *EFEMP2* encodes a smaller *in vitro* translated form (Gallagher et al. 2001). The smaller protein form was shown to have no signal sequence based on a solubility and proteinase test (Gallagher et al. 2001). Based on this evidence, Gallagher *et al.* proposed that an intracellular form of EFEMP2 is encoded using methionine 69 as an alternate translation start site (figure 4-2). This proposed intracellular form of EFEMP2 is entirely encoded within the $EFEMP2_{\Delta N36}$ clone identified in this study. A closely related gene, EFEMP1, may also encode protein isoforms without a signal sequence (Lecka-Czernik et al. 1995).

There may also be another start methionine upstream of the putative EFEMP2 signal sequence. The 5' sequence of EFEMP2 is not defined (figure 4-2). Since the known cDNA sequence does not contain an in-frame stop codon upstream of the human signal peptide methionine, it is possible that there could be another upstream translational start to encode a cellular form. Translation of the genomic sequence upstream of EFEMP2 reveals an in-frame start codon approximately 130 amino acids upstream of the signal sequence and an in-frame stop codon upstream of that potential start site (figure 4-2).

Fibulin protein interaction research has also provided support for an intracellular EFEMP2 role. Prior to this study, the only other protein that has been experimentally verified to interact with EFEMP2 is mutant p53 (Gallagher et al.

1999). Like PITX2, p53 is nuclear transcription factor that contains DNA-binding and transcription activation domains. In particular, EFEMP2 was found to strongly bind structural mutants of p53 that are conformationally different than the wildtype protein. The mutant p53/EFEMP2 interaction occurs in the absence of EFEMP2's N-terminus (figure 4-2), so the mutant p53 interaction domain within EFEMP2 may be close to or the same as the PITX2 interaction domain. This study went on to show EFEMP2 and mutant p53 having a functional oncogenic synergistic interaction, which occured with or without EFEMP2's putative signal sequence. Unlike other fibulin family members, EFEMP2 has not been found to bind ECM or membrane proteins (table 4-1).

Even if an alternate form of the EFEMP2 protein does not exist, the signal-peptide form of the protein is still likely to be available for an intracellular protein-protein interaction. The 443 amino acid form of the EFEMP2 protein contains a putative signal peptide. Giltay *et al.* have shown that EFEMP2 is not secreted well with its own signal sequence (Giltay et al. 1999). This result may or may not be due to a polymorphism found in the EFEMP2 signal peptide consensus (Gallagher et al. 2001). Another fibulin protein similar to EFEMP2 (Fibulin 5) has also been shown to be poorly secreted (Kowal et al. 1999b). Only a small portion of a full length fibulin-5 C-terminal Myc tagged protein was found to be secreted and the majority of the protein localized within the cell including some nuclear localization (Kowal et al. 1999b). The localization of full length fibulin-5 in COS cells is very similar to the localization of $EFEMP2_{\Delta N36}$ in COS-7 cells demonstrated in this study. These results indicate that EFEMP2's putative signal peptide may not prevent intracellular retention of EFEMP2.

An intracellular EFEMP2/PITX2 interaction may affect the transactivational function of PITX2. This is particularly true if the EFEMP2/PITX2 interaction is occurring in the transcriptionally active regions of the nucleus as demonstrated with the $EFEMP2_{\Delta N36}$/PITX2. The PITX2/EFEMP2 protein-protein interaction could be regulating PITX2 transcriptional activity in the HTM in a manner analogous to the PITX2/PIT-1 interaction occurring in the pituitary gland (Amendt et al. 1999).

This study has shown that the localization of the EFEMP2 $_{\Delta N36}$ protein can be altered by an interaction with PITX2. The converse may also be true. If a form of the EFEMP2 protein is secreted, the EFEMP2/PITX2 complex could target PITX2 outside the cell. This leads to another equally exciting, but not mutually exclusive, biological interaction hypothesis (figure 4-3).

While there is little direct evidence that PITX2 leaves the cell, there is an emerging school of thought for paracrine functions of transcription factors. Transcription factors and in particular, homeoproteins, are hypothesized to be exported from cells and be internalized into neighboring cells (Prochiantz and Joliot 2003). The transcription factor export mechanism remains unclear. An interaction model proposed for the EFEMP2/mutant p53 interaction is that these two proteins meet in lumen of the endoplasmic reticulum as EFEMP2 is moving through the secretory pathway (Gallagher et al. 2001). PITX2 possesses sequences that correspond to the homeodomain cellular import and export consensus sequences, but until more direct evidence is uncovered, this model remains highly speculative. It is possible that a PITX2/EFEMP2 protein-protein interaction can target PITX2 to a secretory pathway and subsequent intercellular transfer. The secretory ability of a PITX2/EFEMP2 complex can be tested as described in Chapter Five.

The information I have presented and discussed in this section raises the possibility that different EFEMP2 protein forms can be produced and that the PITX2/EFEMP2 interaction can have different biological functions depending on the EFEMP2 form involved. Different EFEMP2 protein forms may be tissue specific and can provide an explanation of how it would be possible to have a human disease phenotype involving these genes manifested in limited tissues (e.g. ocular tissues) while both PITX2 and EFEMP2 are widely expressed.

I would suggest to the Human Genome Organization (HUGO) nomenclature committee that the fibulin-4 term be used to describe the EFEMP2 gene and gene products. The name 'EGF-containing fibulin-like extracellular matrix protein 2', does not reflect the potential intracellular role of the protein.

Relevance of a PITX2/EFEMP2 interaction in ARS

I have shown that PITX2 can affect the intracellular localization of $EFEMP2_{\Delta N36}$, indicating a functional affect of a PITX2/EFEMP2 interaction. EFEMP2 interacts with PITX2 outside of the PITX2 homeodomain (figure 3-6). The majority of PITX2 missense mutations occur within the homeodomain and therefore would not be expected to directly affect the PITX2/EFEMP2 interaction. ARS nonsense or frameshift mutations that cause a PITX2 truncation may negate a PITX2/EFEMP2 interaction. If EFEMP2 is unable to interact with mutant PITX2 proteins, then EFEMP2 nuclear translocation would be eliminated and any potential EFEMP2 mediated transcriptional regulation of PITX2 would not occur. The converse is also true in that mutations in *EFEMP2* may negate the PITX2/EFEMP2 interaction and cause a disease phenotype. Affects of ARS mutations on this interaction need to be tested directly to define the significance of this interaction in ARS pathogenesis. More research is necessary to uncover how the PITX2/EFEMP2 interaction relates to ARS pathogenesis.

***EFEMP2* is a candidate gene for glaucoma**

EFEMP2 does not share a genomic map location with any mapped ARS loci, but remains a candidate gene for unmapped and sporadic ARS phenotypes. Interestingly, *EFEMP2* does lie within the critical region of a nanophthalmos locus (NNO1) (Othman et al. 1998) and in close proximity to the provisional microcornea, rod cone dystrophy, cataract and posterior staphloma (MRCS) locus. MRCS is postulated to be an allelic variant of NNO1 (Reddy et al. 2003).

Like ARS, nanophthalmos exhibits autosomal dominant inheritance of congential anterior chamber malformations accompanied by a high rate of glaucoma. NNO is associated with angle closure glaucoma (ACG). The ACG phenotype is described as a narrow or occludable drainage angle, accompanied by glaucomatous optic neuropathy (Aung and Chew 2002). Linkage analysis in one family assigned the locus of the ocular defect (NNO1) to chromosome 11 in a 14.7-cM interval. Of the 22 affected family members, twelve had angle-closure glaucoma or occludable anterior-chamber angles (Othman et al. 1998). Another autosomal dominant NNO

loci (NNO2) has been identified at 15q12-q15 (Morle et al. 2000), and an autosomal recessive form has been mapped to 14q32 (OMIM %251600). Interestingly, fibulin 5 maps to 14q32.1 (Kowal et al. 1999a). The demonstrated PITX2/EFEMP2 protein-protein interaction and the phenotypic similarity of NNO to ARS make *EFEMP2* an attractive candidate gene for NNO1.

EFEMP2 can also be considered a glaucoma candidate gene because it parallels the known glaucoma genes, *MYOC* and *OPTN*. Like *EFEMP2*, *MYOC* and *OPTN* both encode secreted proteins that are expressed in the trabecular meshwork (Caballero et al. 2000; Jacobson et al. 2001; Rezaie et al. 2002; Sarfarazi and Rezaie 2003; Tomarev et al. 2003). In the case of OPTN, similarities to EFEMP2 continue. OPTN has been found to bind a transcription factor (TFIIIA) (Moreland et al. 2000), as EFEMP2 has been found to bind a transcription factor (PITX2) in this study. These similarities to known glaucoma genes provide further evidence to consider *EFEMP2* as a glaucoma candidate gene.

Secondary conclusions

In addition to the identification of a novel PITX2 protein interaction, this study has also revealed secondary information.

CytoTrap library conclusions

The CytoTrap two-hybrid system (Stratagene) is a variation of the yeast two-hybrid system. In order to discover PITX2 interacting proteins (PIPs) and important HTM genes, I attempted to create a HTM yeast two-hybrid cDNA library in the CytoTrap system. In order to facilitate downstream applications of identified PITX2 interaction proteins, I modified the cDNA cloning system to include GATEWAY-compatible sequences. Because the library creation system was experimental, the first library creation attempt was performed using easily obtainable porcine RNA.

With only 10^2-10^4 pcfu per library, the modified CytoTrap library construction protocol did not produce libraries representative of a transcriptome. The low number of pcfu produced with this system was most-likely due an over-estimation of the amount of poly-A RNA used as starting material combined with

sub-optimal ligation and transformation efficiencies. Commercially available cDNA libraries contain a much higher number of pcfu. Standard cDNA libraries available from Invitrogen contain $>10_7$ primary clones and two-hybrid libraries contain >5 x 10^6 primary clones to ensure representation and presence of rare sequences. The modified CytoTrap library creation efficiency was not high enough to warrant the creation of a HTM library within this system. Therefore, a commercial cDNA library creation service with guaranteed results was used to construct the HTM library.

PITX2 dimerization

PITX2 dimerization has been demonstrated in the Matchmaker3 Y2H system (Clonetech)(Saadi et al. 2003) and by co-immunoprecipitation (Matthew Lines personal communication). Unlike these two methods, the ProQuest Y2H system used in this study is not a protein overexpression system. I have tested the PITX2 dimerization interaction directly and found that PITX2 does not interact with itself to activate in the ProQuest two-hybrid system. The lack of PITX2 dimer detection shown here, demonstrates that the ProQuest CEN-based system is less sensitive than the overexpression methods. The advantage of this lowered sensitivity allows the reduction of false positive interactions occurring during Y2H screening. Therefore, positive interaction results in the ProQuest system are more likely to be true interactions, but some real interactions may be missed (false negatives).

HTM Y2H library screen analysis

While doing the Y2H library screen I have demonstrated that co-transformant yeast colonies appearing on media lacking histidine after four days of incubation are false positives and need not be examined further. By limiting analysis of co-transformant colonies to those growing within four days of plating, unnecessary experimental time can be eliminated.

Within the ProQuest Y2H system, the URA reporter gene promoter contains an upstream repressor sequence (URS1). The URS makes the reciprocal URA/5FOA phenotypes less sensitive to activation and therefore more stringent selection criteria. Lack of co-transformant growth on media without uracil combined with a HIS+, X-

gal+ phenotype, categorizes a protein-protein interaction as a probable weak interaction. It is possible that the PITX2/EFEMP2 interaction is yeast is weaker without the presence of mammalian post-translational modifications. There is variability in the amount of 5FOA growth inhibition displayed by the different sized EFEMP2 co-transformants (Table 3-1). These differences may represent a variation of the strength of PITX2 interaction with different lengths of EFEMP2 clones or may be an artifactual result of inconsistent replica plating and replica cleaning techniques. The true cause is difficult to determine.

PITX2/EFEMP2 interaction domain mapping

Initial PITX2/EFEMP2 interaction domain mapping results indicate that EFEMP2 interacts specifically with PITX2 outside of the homeodomain (figure 3-6). The shortest EFEMP2 clone identified by the Y2H screen (2P141 aka $EFEMP2_{\Delta N134}$) only encodes the C-terminal 309 AA of EFEMP2 (figure 4-2). This suggests that the N-terminal portion of EFEMP2 is not required for a PITX2 interaction. These results will need to be confirmed and refined within a mammalian system, possibly using a co-IP experiment.

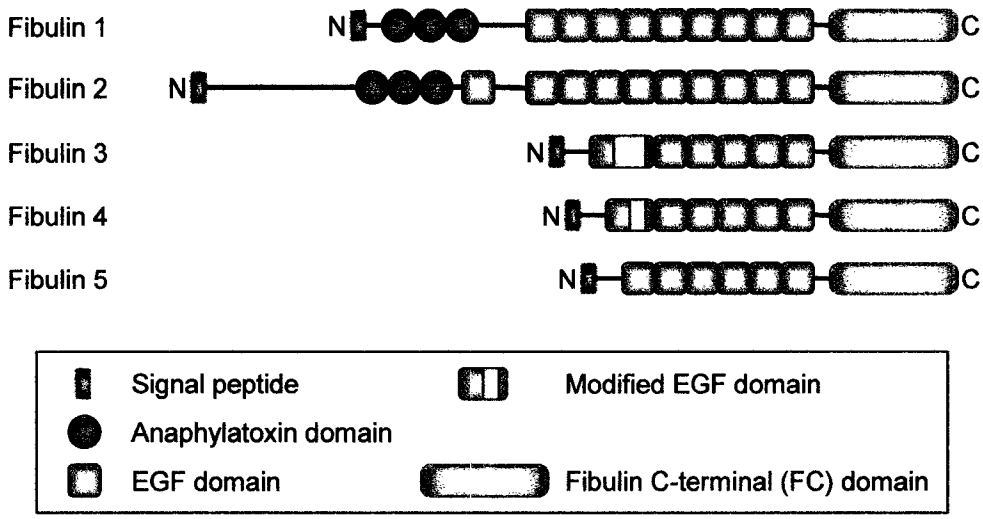

Table 4-1: Fibulin protein-protein interactions (Chu and Tsuda 2004)

Ligands	FBLN1	FBLN2	FBLN4	FBLN5
Fibronectin				
Elastic fiber	+	+		
Tropoelastin	+	+		+
Fibrillin-1		+		
Fibulin-1	+			
Endostatin (collagen XVIII)	+	+		
Nidogen-2		+		
Basement membrane				
Nidogen-1	+	+		
Laminin α1 chain	+			
Laminin α2 chain	+	+		
Laminin γ2 chain	+	+		
Perlecan		+		
Integrin				
α1bβ3		+		
αvβ3		+		+
αvβ5				+
α9β1				+
Letican proteoglycan				
Versican	+	+		
Aggrecan	+	+		
Others				
Fibrinogen	+			
Connective tissue growth factor	+			
HB-EGF growth factor	+			
β-amyloid precursor protein	+			
Mutant p53			+	

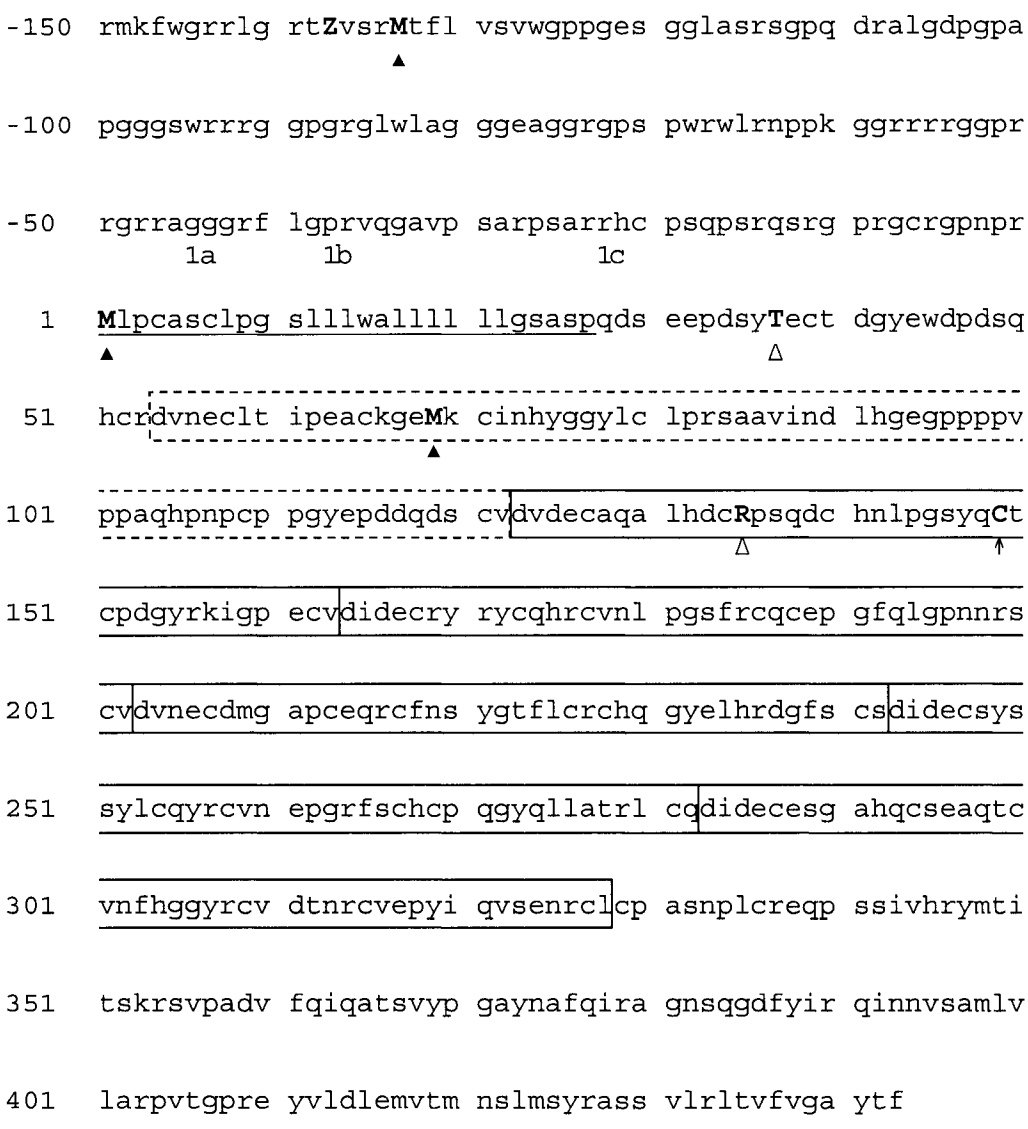

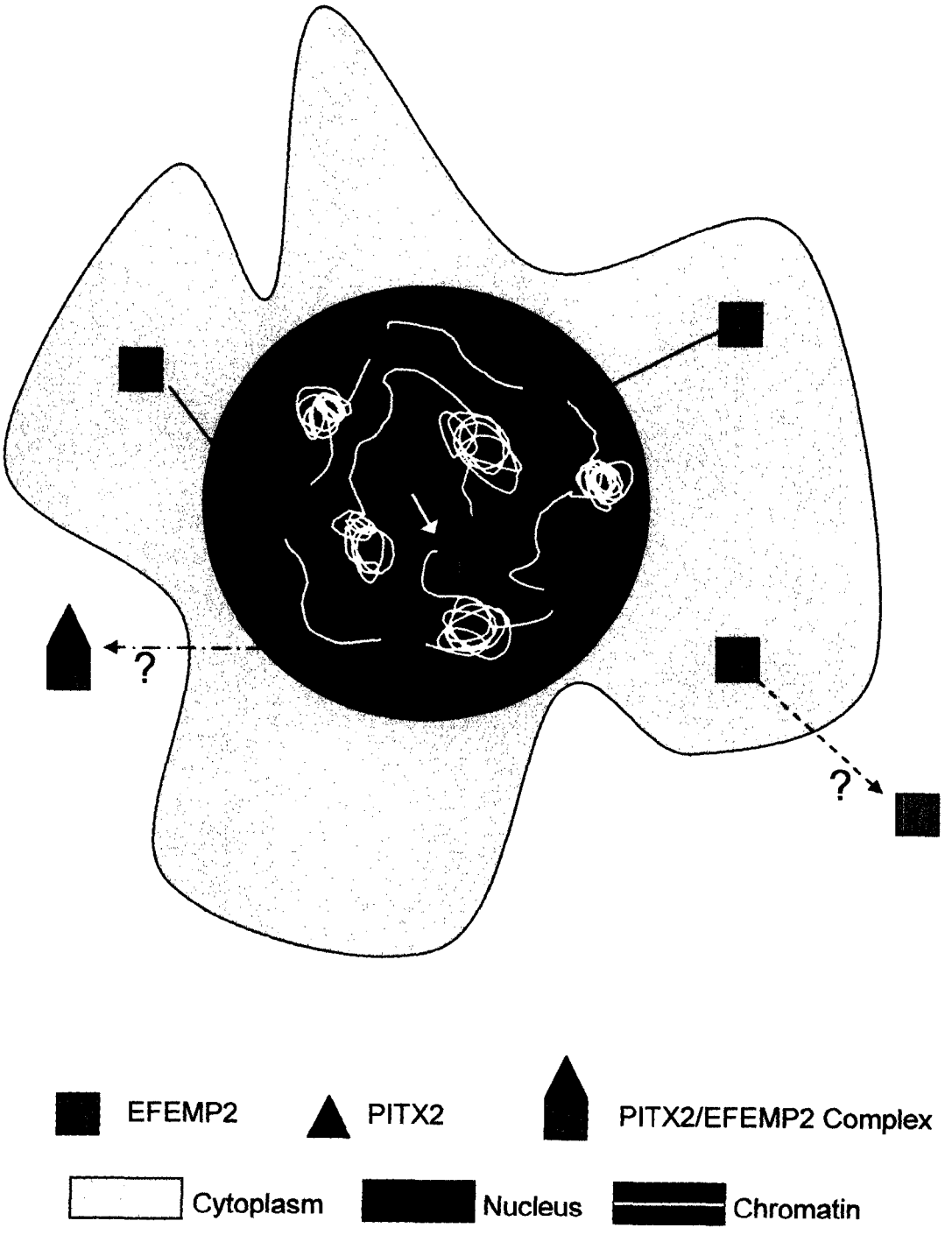

Chapter Five: Future Directions

Further identification of PITX2 interacting proteins

While screening the HTM library with PITX2, I did not reach levels of screening saturation. A screen of millions of co-transformants would be needed to ensure coverage of the HTM transcriptome. A higher Y2H screening efficiency may be reached by sequentially transforming the bait and prey entities into the yeast instead of co-transforming them. Continued Y2H screening of the HTM library can identify additional PITX2 interacting proteins. Repeated PITX2 screening of the HTM library should use a method to identify or eliminate EFEMP2 clones in order to reduce laborious further characterization of non-novel PITX2 interactions. Identification of EFEMP2 containing colonies can be accomplished by a colony filter lift or colony PCR method. To identify PITX2 protein-protein interactions specific to developmental tissues, a screen could be done on ProQuest 8.5 or 10.5 day mouse embryo cDNA libraries available for commercial purpose (Invitrogen, catalog numbers: 11291-010 and 11292-018).

The yeast colony I have identified as 2P061 is possibly a mixed population of prey proteins that includes empty vector and an interacting prey construct. Other yeast colonies examined in this study were discovered to be mixed populations of EFEMP2 clones and empty vector (data not shown). If more bacterial 2P061 clones were sequenced, a cDNA insert can possibly be identified. Additional bacterial clone sequencing will reveal the identity of 2P061 as a mixed population or a false positive with no cDNA inserts. Identification of a 2P061 prey protein can be validated using the methods described to determine if it is a PITX2 interacting protein.

Defining EFEMP2 protein forms

There are several possible reasons why a full length, 443 amino acid, EFEMP2 clone was not identified during the library screen. The most obvious explanations for this are that not enough co-transformants were screened, or a full-length transcript was not cloned in the library. A third possibility is that the HTM only transcribes the proposed intracellular form of EFEMP2. The proposed intracellular form is completely encoded by the 2P151, 2P152, and 2P161 clones.

Finally, the fusion protein encoding a full length EFEMP2 protein may be secreted from the yeast cell and these prey proteins would have no opportunity to activate the reporter genes.

Northern blot analysis of HTM RNA probed with an EFEMP2 probe will determine the transcript sizes of EFEMP2 in the TM. Northern analysis may also reveal HTM specific transcripts. Performing 5'-RACE (rapid amplification of cDNA ends) (Matz et al. 1999) on the HTM cell culture RNA would help identify EFEMP2 splice variants. RACE can allow us to define and obtain a copy of the full length EFEMP2 transcript expressed in the HTM. RACE results may also reveal the identity of upstream exons in the *EFEMP2* gene. The locations of upstream exons can potentially expand the mapping location of EFEMP2 and make it a candidate gene for more disease phenotypes. Katsanis *et al.* attempted 5'-RACE but were unsuccessful (Katsanis et al. 2000). Failure was attributed to the high GC percentage in EFEMP2's 5' UTR. This problem may be alleviated by using commercial kits designed for templates of high GC content.

Further characterization of the EFEMP2/PITX2 interaction

If the full length HTM EFEMP2 ORF length is determined to be different than the $EFEMP2_{\Delta N36}$ ORF length, it would be interesting to see if a full length HTM EFEMP2 protein localizes differently within the cell. The intracellular localization could be tested by repeating the immunofluorescence and co-immunofluorescence described with a full length HTM EFEMP2 construct. The intracellular localization of fibulin-5 with a signal sequence (Kowal et al. 1999b) is similar to the localization of $EFEMP2_{\Delta N36}$ (figure 3-9). This suggests that a construct encoding EFEMP2 with a signal sequence still may not have a different intracellular localization than that seen for $EFEMP2_{\Delta N36}$.

It is possible that PITX2 would even bind a secreted form of EFEMP2 before it leaves the cell and piggy-back EFEMP2 into the nucleus. But, if full length EFEMP2/PITX2 co-localization is different than $EFEMP2_{\Delta N36}$/PITX2 co-localization, immunoblot analysis can be used to test for the presence of EFEMP2 and PITX2 in the culture media. If a higher quantity of PITX2 is detected in the culture media

when EFEMP2 is co-expressed with PITX2 than without EFEMP2, EFEMP2 is aiding in PITX2 export from the cell.

An EFEMP2 antibody has been made against human EFEMP2 that cross reacts with mouse Efemp2 (Giltay et al. 1999). This antibody can be used for identification of endogenous EFEMP2 tissue expression within the eye and anterior chamber and endogenous intracellular localization in HTM cells. The EFEMP2 antibody could also be used to determine the size of the endogenous EFEMP2 protein in the eye by protein extractions and immunoblot analysis. In combination with the attainment of a functional PITX2 antibody, an EFEMP2 antibody can be used to study PITX2/EFEMP2 interaction in HTM cells and ocular tissues. Detection of an EFEMP2/PITX2 interaction occurring within ocular tissues and cells would be a final proof of this interaction occurring in a biologically relevant manner.

Initial interaction domain mapping evidence indicates that EFEMP2 interacts with PITX2 outside of the PITX2 homeodomain. This would mean that PITX2 ARS missense mutations in the homeodomain would not necessarily affect EFEMP2 binding. If EFEMP2 is found to bind PITX2 C-terminal region, ARS frameshifts, deletions and nonsense mutations would affect the area that EFEMP2 binds and negate the interaction. A negated PITX2/EFEMP2 interaction may provide an ARS disease mechanism. Mapping of the protein-protein interaction domains will further characterize the PITX2/EFEMP2 interaction.

Because $EFEMP2_{\Delta N36}$ interacts with PITX2 in transcriptionally active regions of the nucleus, it is possible that PITX2's transactivation function is affected by the interaction. An EFEMP2 mediated affect on the transactivation activity of PITX2 can be tested directly with a transactivation assay. If the EFEMP2 interaction is mediated by the C-terminal region of PITX2, then transcriptional activation could be up-regulated similar to PIT-1 binding (Amendt et al. 1999). In summary, further characterization of the EFEMP2/PITX2 interaction will provide insight for the role of an EFEMP2/PITX2 interaction in ARS and glaucoma.

EFEMP2 as an ocular disease candidate gene

Screening of an ARS patient panel for *EFEMP2* mutations is currently in progress. Screening of NNO1 patient DNA will be performed as patient DNA becomes available to us. Patient mutations discovered in *EFEMP2* can be modeled in cell culture to determine whether or not the mutation has an effect on the EFEMP2/PITX2 interaction or on EFEMP2 cellular localization. This information can provide us with insight into ARS and glaucoma pathogenesis.

Final comments

In summary, I have identified EFEMP2 as a PITX2 interacting protein though a Y2H screen of a HTM cDNA library. Within the Y2H system, I have determined that EFEMP2 interacts with PITX2 specifically and outside of the PITX2 homeodomain. I have confirmed the EFEMP2/PITX2 interaction within a mammalian system through co-immunoprecipitation and co-immunoflouresence experiments. EFEMP2 and PITX2 are co-expressed in several human tissues and therefore could interact in a biologically relevant manner. The functional relevance of the EFEMP2/PITX2 interaction may involve proper protein localization of EFEMP2 through nuclear translocation and/or the trafficking of PITX2 outside of the cell. Based on my results and the map location of the *EFEMP2* gene, *EFEMP2* is an attractive candidate gene for ocular disorders including NNO1. My research has opened several interesting avenues for further research.

References

Acott TS, Westcott M, Passo MS, Van Buskirk EM (1985) Trabecular meshwork glycosaminoglycans in human and cynomolgus monkey eye. Invest Ophthalmol Vis Sci 26:1320-1329

Akarsu AN, Turacli ME, Aktan SG, Barsoum-Homsy M, Chevrette L, Sayli BS, Sarfarazi M (1996) A second locus (GLC3B) for primary congenital glaucoma (Buphthalmos) maps to the 1p36 region. Hum Mol Genet 5:1199-1203

Alexander JP, Samples JR, Van Buskirk EM, Acott TS (1991) Expression of matrix metalloproteinases and inhibitor by human trabecular meshwork. Invest Ophthalmol Vis Sci 32:172-180

Alvarado J, Murphy C, Juster R (1984) Trabecular meshwork cellularity in primary open-angle glaucoma and nonglaucomatous normals. Ophthalmology 91:564-579

Alward WL (2000) Axenfeld-Rieger syndrome in the age of molecular genetics. Am J Ophthalmol 130:107-115

Alward WL, Semina EV, Kalenak JW, Heon E, Sheth BP, Stone EM, Murray JC (1998) Autosomal dominant iris hypoplasia is caused by a mutation in the Rieger syndrome (RIEG/PITX2) gene. Am J Ophthalmol 125:98-100

Amendt BA, Sutherland LB, Russo AF (1999) Multifunctional role of the Pitx2 homeodomain protein C-terminal tail. Mol Cell Biol 19:7001-7010

Amendt BA, Sutherland LB, Semina EV, Russo AF (1998) The molecular basis of Rieger syndrome. Analysis of Pitx2 homeodomain protein activities. J Biol Chem 273:20066-20072

Argraves WS, Dickerson K, Burgess WH, Ruoslahti E (1989) Fibulin, a novel protein that interacts with the fibronectin receptor beta subunit cytoplasmic domain. Cell 58:623-629

Argraves WS, Greene LM, Cooley MA, Gallagher WM (2003) Fibulins: physiological and disease perspectives. EMBO Rep 4:1127-1131

Aung T, Chew PT (2002) Review of recent advancements in the understanding of primary angle-closure glaucoma. Curr Opin Ophthalmol 13:89-93

Bach I, Carriere C, Ostendorff HP, Andersen B, Rosenfeld MG (1997) A family of LIM domain-associated cofactors confer transcriptional synergism between LIM and Otx homeodomain proteins. Genes Dev 11:1370-1380

Berry FB, Saleem RA, Walter MA (2002) FOXC1 transcriptional regulation is mediated by N- and C-terminal activation domains and contains a phosphorylated transcriptional inhibitory domain. J Biol Chem 277:10292-10297

Borges AS, Susanna R, Jr., Carani JC, Betinjane AJ, Alward WL, Stone EM, Sheffield VC, Nishimura DY (2002) Genetic analysis of PITX2 and FOXC1 in Rieger Syndrome patients from Brazil. J Glaucoma 11:51-56

Borras T (2003) Gene expression in the trabecular meshwork and the influence of intraocular pressure. Prog Retin Eye Res 22:435-463

Bradford AP, Wasylyk C, Wasylyk B, Gutierrez-Hartmann A (1997) Interaction of Ets-1 and the POU-homeodomain protein GHF-1/Pit-1 reconstitutes pituitary-specific gene expression. Mol Cell Biol 17:1065-1074

Bron AJ, Tripathi RC, Tripathi BJ (1997) Wolff's Anatomy of the Eye and Orbit. Chapman & Hall Medical, New York

Brooks BP, Moroi SE, Downs CA, Wiltse S, Othman MI, Semina EV, Richards JE (2004) A novel mutation in the PITX2 gene in a family with Axenfeld-Rieger syndrome. Ophthalmic Genet 25:57-62

Caballero M, Rowlette LL, Borras T (2000) Altered secretion of a TIGR/MYOC mutant lacking the olfactomedin domain. Biochim Biophys Acta 1502:447-460

Carpenter G, Cohen S (1990) Epidermal growth factor. J Biol Chem 265:7709-7712

Chanda V (1995) Current Protocols in Molecular Biology. Vol 1. John Wiley & Sons, Inc., United States of America

Chevray PM, Nathans D (1992) Protein interaction cloning in yeast: identification of mammalian proteins that react with the leucine zipper of Jun. Proc Natl Acad Sci U S A 89:5789-5793

Chu ML, Tsuda T (2004) Fibulins in development and heritable disease. Birth Defects Res Part C Embryo Today 72:25-36

Durocher D, Charron F, Warren R, Schwartz RJ, Nemer M (1997) The cardiac transcription factors Nkx2-5 and GATA-4 are mutual cofactors. Embo J 16:5687-5696

Ethier CR, Kamm RD, Palaszewski BA, Johnson MC, Richardson TM (1986) Calculations of flow resistance in the juxtacanalicular meshwork. Invest Ophthalmol Vis Sci 27:1741-1750

Fields S, Song O (1989) A novel genetic system to detect protein-protein interactions. Nature 340:245-246

Foster PJ, Johnson GJ (2001) Glaucoma in China: how big is the problem? Br J Ophthalmol 85:1277-1282

Freddo TF, Patterson MM, Scott DR, Epstein DL (1984) Influence of mercurial sulfhydryl agents on aqueous outflow pathways in enucleated eyes. Invest Ophthalmol Vis Sci 25:278-285

Friedman JS, Walter MA (1999) Glaucoma genetics, present and future. Clin Genet 55:71-79

Furukawa T, Kozak CA, Cepko CL (1997) rax, a novel paired-type homeobox gene, shows expression in the anterior neural fold and developing retina. Proc Natl Acad Sci U S A 94:3088-3093

Gage PJ, Suh H, Camper SA (1999) Dosage requirement of Pitx2 for development of multiple organs. Development 126:4643-4651

Gallagher WM, Argentini M, Sierra V, Bracco L, Debussche L, Conseiller E (1999) MBP1: a novel mutant p53-specific protein partner with oncogenic properties. Oncogene 18:3608-3616

Gallagher WM, Greene LM, Ryan MP, Sierra V, Berger A, Laurent-Puig P, Conseiller E (2001) Human fibulin-4: analysis of its biosynthetic processing and mRNA expression in normal and tumour tissues. FEBS Lett 489:59-66

Giltay R, Timpl R, Kostka G (1999) Sequence, recombinant expression and tissue localization of two novel extracellular matrix proteins, fibulin-3 and fibulin-4. Matrix Biol 18:469-480

Gong H, Ruberti J, Overby D, Johnson M, Freddo TF (2002) A new view of the human trabecular meshwork using quick-freeze, deep-etch electron microscopy. Exp Eye Res 75:347-358

Gonzalez P, Epstein DL, Borras T (2000) Characterization of gene expression in human trabecular meshwork using single-pass sequencing of 1060 clones. Invest Ophthalmol Vis Sci 41:3678-3693

Hanes SD, Brent R (1989) DNA specificity of the bicoid activator protein is determined by homeodomain recognition helix residue 9. Cell 57:1275-1283

Hassan B, Li L, Bremer KA, Chang W, Pinsonneault J, Vaessin H (1997) Prospero is a panneural transcription factor that modulates homeodomain protein activity. Proc Natl Acad Sci U S A 94:10991-10996

Heine H, Delude RL, Monks BG, Espevik T, Golenbock DT (1999) Bacterial lipopolysaccharide induces expression of the stress response genes hop and H411. J Biol Chem 274:21049-21055

Hjalt TA, Semina EV, Amendt BA, Murray JC (2000) The Pitx2 protein in mouse development. Dev Dyn 218:195-200

Jacobson N, Andrews M, Shepard AR, Nishimura D, Searby C, Fingert JH, Hageman G, Mullins R, Davidson BL, Kwon YH, Alward WL, Stone EM, Clark AF, Sheffield VC (2001) Non-secretion of mutant proteins of the glaucoma gene myocilin in cultured trabecular meshwork cells and in aqueous humor. Hum Mol Genet 10:117-125

Katsanis N, Venable S, Smith JR, Lupski JR (2000) Isolation of a paralog of the Doyne honeycomb retinal dystrophy gene from the multiple retinopathy critical region on 11q13. Hum Genet 106:66-72

Kidson SH, Kume T, Deng K, Winfrey V, Hogan BL (1999) The forkhead/winged-helix gene, Mfl, is necessary for the normal development of the cornea and formation of the anterior chamber in the mouse eye. Dev Biol 211:306-322

Kioussi C, Briata P, Baek SH, Rose DW, Hamblet NS, Herman T, Ohgi KA, Lin C, Gleiberman A, Wang J, Brault V, Ruiz-Lozano P, Nguyen HD, Kemler R, Glass CK, Wynshaw-Boris A, Rosenfeld MG (2002) Identification of a Wnt/Dvl/beta-Catenin --> Pitx2 pathway mediating cell-type-specific proliferation during development. Cell 111:673-685

Klenotic PA, Munier FL, Marmorstein LY, Anand-Apte B (2004) Tissue Inhibitor of Metalloproteinases-3 (TIMP-3) Is a Binding Partner of Epithelial Growth Factor-containing Fibulin-like Extracellular Matrix Protein 1 (EFEMP1): IMPLICATIONS FOR MACULAR DEGENERATIONS. J Biol Chem 279:30469-30473

Kowal RC, Jolsin JM, Olson EN, Schultz RA (1999a) Assignment of fibulin-5 (FBLN5) to human chromosome 14q31 by in situ hybridization and radiation hybrid mapping. Cytogenet Cell Genet 87:2-3

Kowal RC, Richardson JA, Miano JM, Olson EN (1999b) EVEC, a novel epidermal growth factor-like repeat-containing protein upregulated in embryonic and diseased adult vasculature. Circ Res 84:1166-1176

Kozlowski K, Walter MA (2000) Variation in residual PITX2 activity underlies the phenotypic spectrum of anterior segment developmental disorders. Hum Mol Genet 9:2131-2139

Kulak SC, Kozlowski K, Semina EV, Pearce WG, Walter MA (1998) Mutation in the RIEG1 gene in patients with iridogoniodysgenesis syndrome. Hum Mol Genet 7:1113-1117

Larsson C, Hellqvist M, Pierrou S, White I, Enerback S, Carlsson P (1995) Chromosomal localization of six human forkhead genes, freac-1 (FKHL5), -3 (FKHL7), -4 (FKHL8), -5 (FKHL9), -6 (FKHL10), and -8 (FKHL12). Genomics 30:464-469

Lecka-Czernik B, Lumpkin CK, Jr., Goldstein S (1995) An overexpressed gene transcript in senescent and quiescent human fibroblasts encoding a novel protein in the epidermal growth factor-like repeat family stimulates DNA synthesis. Mol Cell Biol 15:120-128

Lin CR, Kioussi C, O'Connell S, Briata P, Szeto D, Liu F, Izpisua-Belmonte JC, Rosenfeld MG (1999) Pitx2 regulates lung asymmetry, cardiac positioning and pituitary and tooth morphogenesis. Nature 401:279-282

Lines MA, Kozlowski K, Kulak SC, Allingham RR, Heon E, Ritch R, Levin AV, Shields MB, Damji KF, Newlin A, Walter MA (2004) Characterization and prevalence of PITX2 microdeletions and mutations in Axenfeld-Rieger malformations. Invest Ophthalmol Vis Sci 45:828-833

Lines MA, Kozlowski K, Walter MA (2002) Molecular genetics of Axenfeld-Rieger malformations. Hum Mol Genet 11:1177-1184

Lu MF, Pressman C, Dyer R, Johnson RL, Martin JF (1999) Function of Rieger syndrome gene in left-right asymmetry and craniofacial development. Nature 401:276-278

Matz M, Shagin D, Bogdanova E, Britanova O, Lukyanov S, Diatchenko L, Chenchik A (1999) Amplification of cDNA ends based on template-switching effect and step-out PCR. Nucleic Acids Res 27:1558-1560

Mears AJ, Jordan T, Mirzayans F, Dubois S, Kume T, Parlee M, Ritch R, Koop B, Kuo WL, Collins C, Marshall J, Gould DB, Pearce W, Carlsson P, Enerback S, Morissette J, Bhattacharya S, Hogan B, Raymond V, Walter MA (1998) Mutations of the forkhead/winged-helix gene, FKHL7, in patients with Axenfeld-Rieger anomaly. Am J Hum Genet 63:1316-1328

Mears AJ, Mirzayans F, Gould DB, Pearce WG, Walter MA (1996) Autosomal dominant iridogoniodysgenesis anomaly maps to 6p25. Am J Hum Genet 59:1321-1327

Modrell B, McDonald VL, Shoyab M (1992) The interaction of amphiregulin with nuclei and putative nuclear localization sequence binding proteins. Growth Factors 7:305-314

Moreland RJ, Dresser ME, Rodgers JS, Roe BA, Conaway JW, Conaway RC, Hanas JS (2000) Identification of a transcription factor IIIA-interacting protein. Nucleic Acids Res 28:1986-1993

Morle L, Bozon M, Zech JC, Alloisio N, Raas-Rothschild A, Philippe C, Lambert JC, Godet J, Plauchu H, Edery P (2000) A locus for autosomal dominant

colobomatous microphthalmia maps to chromosome 15q12-q15. Am J Hum Genet 67:1592-1597

Othman MI, Sullivan SA, Skuta GL, Cockrell DA, Stringham HM, Downs CA, Fornes A, Mick A, Boehnke M, Vollrath D, Richards JE (1998) Autosomal dominant nanophthalmos (NNO1) with high hyperopia and angle-closure glaucoma maps to chromosome 11. Am J Hum Genet 63:1411-1418

Perveen R, Lloyd IC, Clayton-Smith J, Churchill A, van Heyningen V, Hanson I, Taylor D, McKeown C, Super M, Kerr B, Winter R, Black GC (2000) Phenotypic variability and asymmetry of Rieger syndrome associated with PITX2 mutations. Invest Ophthalmol Vis Sci 41:2456-2460

Phillips JC (2002) Four novel mutations in the PITX2 gene in patients with Axenfeld-Rieger syndrome. Ophthalmic Res 34:324-326

Phillips JC, del Bono EA, Haines JL, Pralea AM, Cohen JS, Greff LJ, Wiggs JL (1996) A second locus for Rieger syndrome maps to chromosome 13q14. Am J Hum Genet 59:613-619

Phizicky EM, Fields S (1995) Protein-protein interactions: methods for detection and analysis. Microbiol Rev 59:94-123

Pinsonneault J, Florence B, Vaessin H, McGinnis W (1997) A model for extradenticle function as a switch that changes HOX proteins from repressors to activators. Embo J 16:2032-2042

Polansky JR, Weinreb RN, Baxter JD, Alvarado J (1979) Human trabecular cells. I. Establishment in tissue culture and growth characteristics. Invest Ophthalmol Vis Sci 18:1043-1049

Polansky JR, Wood IS, Maglio MT, Alvarado JA (1984) Trabecular meshwork cell culture in glaucoma research: evaluation of biological activity and structural properties of human trabecular cells in vitro. Ophthalmology 91:580-595

Priston M, Kozlowski K, Gill D, Letwin K, Buys Y, Levin AV, Walter MA, Heon E (2001) Functional analyses of two newly identified PITX2 mutants reveal a novel molecular mechanism for Axenfeld-Rieger syndrome. Hum Mol Genet 10:1631-1638

Prochiantz A, Joliot A (2003) Can transcription factors function as cell-cell signalling molecules? Nat Rev Mol Cell Biol 4:814-819

Quigley HA (1996) Number of people with glaucoma worldwide. Br J Ophthalmol 80:389-393

Quigley HA, Vitale S (1997) Models of open-angle glaucoma prevalence and incidence in the United States. Invest Ophthalmol Vis Sci 38:83-91

Racette L, Wilson MR, Zangwill LM, Weinreb RN, Sample PA (2003) Primary open-angle glaucoma in blacks: a review. Surv Ophthalmol 48:295-313

Rao Z, Handford P, Mayhew M, Knott V, Brownlee GG, Stuart D (1995) The structure of a Ca(2+)-binding epidermal growth factor-like domain: its role in protein-protein interactions. Cell 82:131-141

Reddy MA, Francis PJ, Berry V, Bradshaw K, Patel RJ, Maher ER, Kumar R, Bhattacharya SS, Moore AT (2003) A clinical and molecular genetic study of a rare dominantly inherited syndrome (MRCS) comprising of microcornea, rod-cone dystrophy, cataract, and posterior staphyloma. Br J Ophthalmol 87:197-202

Rezaie T, Child A, Hitchings R, Brice G, Miller L, Coca-Prados M, Heon E, Krupin T, Ritch R, Kreutzer D, Crick RP, Sarfarazi M (2002) Adult-onset primary open-angle glaucoma caused by mutations in optineurin. Science 295:1077-1079

Saadi I, Kuburas A, Engle JJ, Russo AF (2003) Dominant negative dimerization of a mutant homeodomain protein in Axenfeld-Rieger syndrome. Mol Cell Biol 23:1968-1982

Saadi I, Semina EV, Amendt BA, Harris DJ, Murphy KP, Murray JC, Russo AF (2001) Identification of a dominant negative homeodomain mutation in Rieger syndrome. J Biol Chem 276:23034-23041

Sarfarazi M, Akarsu AN, Hossain A, Turacli ME, Aktan SG, Barsoum-Homsy M, Chevrette L, Sayli BS (1995) Assignment of a locus (GLC3A) for primary congenital glaucoma (Buphthalmos) to 2p21 and evidence for genetic heterogeneity. Genomics 30:171-177

Sarfarazi M, Child A, Stoilova D, Brice G, Desai T, Trifan OC, Poinoosawmy D, Crick RP (1998) Localization of the fourth locus (GLC1E) for adult-onset primary open-angle glaucoma to the 10p15-p14 region. Am J Hum Genet 62:641-652

Sarfarazi M, Rezaie T (2003) Optineurin in primary open angle glaucoma. Ophthalmol Clin North Am 16:529-541

Scully KM, Jacobson EM, Jepsen K, Lunyak V, Viadiu H, Carriere C, Rose DW, Hooshmand F, Aggarwal AK, Rosenfeld MG (2000) Allosteric effects of Pit-1 DNA sites on long-term repression in cell type specification. Science 290:1127-1131

Semenza GL (1998) Transcription Factors and Human Disease. Oxford University Press, New York

Semina EV, Reiter R, Leysens NJ, Alward WL, Small KW, Datson NA, Siegel-Bartelt J, Bierke-Nelson D, Bitoun P, Zabel BU, Carey JC, Murray JC (1996) Cloning and characterization of a novel bicoid-related homeobox transcription factor gene, RIEG, involved in Rieger syndrome. Nat Genet 14:392-399

Sheffield VC, Stone EM, Alward WL, Drack AV, Johnson AT, Streb LM, Nichols BE (1993) Genetic linkage of familial open angle glaucoma to chromosome 1q21-q31. Nat Genet 4:47-50

Shields MB, Buckley E, Klintworth GK, Thresher R (1985) Axenfeld-Rieger syndrome. A spectrum of developmental disorders. Surv Ophthalmol 29:387-409

Srivastava A, MacKay JO, Bell JB (2002) A Vestigial:Scalloped TEA domain chimera rescues the wing phenotype of a scalloped mutation in Drosophila melanogaster. Genesis 33:40-47

Stark MR, Johnson AD (1994) Interaction between two homeodomain proteins is specified by a short C-terminal tail. Nature 371:429-432

Stoilov I, Akarsu AN, Sarfarazi M (1997) Identification of three different truncating mutations in cytochrome P4501B1 (CYP1B1) as the principal cause of primary congenital glaucoma (Buphthalmos) in families linked to the GLC3A locus on chromosome 2p21. Hum Mol Genet 6:641-647

Stoilova D, Child A, Trifan OC, Crick RP, Coakes RL, Sarfarazi M (1996) Localization of a locus (GLC1B) for adult-onset primary open angle glaucoma to the 2cen-q13 region. Genomics 36:142-150

Stone EM, Braun TA, Russell SR, Kuehn MH, Lotery AJ, Moore PA, Eastman CG, Casavant TL, Sheffield VC (2004) Missense variations in the fibulin 5 gene and age-related macular degeneration. N Engl J Med 351:346-353

Stone EM, Fingert JH, Alward WL, Nguyen TD, Polansky JR, Sunden SL, Nishimura D, Clark AF, Nystuen A, Nichols BE, Mackey DA, Ritch R, Kalenak JW, Craven ER, Sheffield VC (1997) Identification of a gene that causes primary open angle glaucoma. Science 275:668-670

Stone EM, Lotery AJ, Munier FL, Heon E, Piguet B, Guymer RH, Vandenburgh K, Cousin P, Nishimura D, Swiderski RE, Silvestri G, Mackey DA, Hageman GS, Bird AC, Sheffield VC, Schorderet DF (1999) A single EFEMP1 mutation associated with both Malattia Leventinese and Doyne honeycomb retinal dystrophy. Nat Genet 22:199-202

Strachan TaR, AP (1999) Human Molecular Genetics 2. BIOS Scientific Publishers, Ltd, Oxford, UK

Tielsch J (1993) Therapy for glaucoma: costs and consequences in glaucoma. CV Mosby, St. Louis

Timpl R, Sasaki T, Kostka G, Chu ML (2003) Fibulins: a versatile family of extracellular matrix proteins. Nat Rev Mol Cell Biol 4:479-489

Toh H (1989) Prostaglandin endoperoxide synthase contains an EGF-like domain. FEBS Lett 258:317-319

Toh H, Yokoyama C, Tanabe T, Yoshimoto T, Yamamoto S (1992) Molecular evolution of cyclooxygenase and lipoxygenase. Prostaglandins 44:291-315

Tolkunova EN, Fujioka M, Kobayashi M, Deka D, Jaynes JB (1998) Two distinct types of repression domain in engrailed: one interacts with the groucho corepressor and is preferentially active on integrated target genes. Mol Cell Biol 18:2804-2814

Tomarev SI, Wistow G, Raymond V, Dubois S, Malyukova I (2003) Gene expression profile of the human trabecular meshwork: NEIBank sequence tag analysis. Invest Ophthalmol Vis Sci 44:2588-2596

Tremblay JJ, Lanctot C, Drouin J (1998) The pan-pituitary activator of transcription, Ptx1 (pituitary homeobox 1), acts in synergy with SF-1 and Pit1 and is an upstream regulator of the Lim-homeodomain gene Lim3/Lhx3. Mol Endocrinol 12:428-441

Trifan OC, Traboulsi EI, Stoilova D, Alozie I, Nguyen R, Raja S, Sarfarazi M (1998) A third locus (GLC1D) for adult-onset primary open-angle glaucoma maps to the 8q23 region. Am J Ophthalmol 126:17-28

Wang Y, Zhao H, Zhang X, Feng H (2003) Novel Identification of a Four-base-pair Deletion Mutation in PITX2 in a Rieger Syndrome Family. J Dent Res 82:1008-1012

Wentz-Hunter K, Ueda J, Yue BY (2002) Protein interactions with myocilin. Invest Ophthalmol Vis Sci 43:176-182

Werner W, Kraft S, Callen DF, Bartsch O, Hinkel GK (1997) A small deletion of 16q23.1-->16q24.2 [del(16)(q23.1q24.2).ish del(16)(q23.1q24.2)(D16S395+,

D16S348-, P5432+)] in a boy with iris coloboma and minor anomalies. Am J Med Genet 70:371-376

Wirtz MK, Samples JR, Kramer PL, Rust K, Topinka JR, Yount J, Koler RD, Acott TS (1997) Mapping a gene for adult-onset primary open-angle glaucoma to chromosome 3q. Am J Hum Genet 60:296-304

Wirtz MK, Samples JR, Rust K, Lie J, Nordling L, Schilling K, Acott TS, Kramer PL (1999) GLC1F, a new primary open-angle glaucoma locus, maps to 7q35-q36. Arch Ophthalmol 117:237-241

Wirtz MK, Samples JR, Xu H, Severson T, Acott TS (2002) Expression profile and genome location of cDNA clones from an infant human trabecular meshwork cell library. Invest Ophthalmol Vis Sci 43:3698-3704

Xu L, Lavinsky RM, Dasen JS, Flynn SE, McInerney EM, Mullen TM, Heinzel T, Szeto D, Korzus E, Kurokawa R, Aggarwal AK, Rose DW, Glass CK, Rosenfeld MG (1998) Signal-specific co-activator domain requirements for Pit-1 activation. Nature 395:301-306

Zhang H, Hu G, Wang H, Sciavolino P, Iler N, Shen MM, Abate-Shen C (1997) Heterodimerization of Msx and Dlx homeoproteins results in functional antagonism. Mol Cell Biol 17:2920-2932